DOI:
10.1016/j.canlet.2020.10.035

Document Version
Peer reviewed version

EGFR Overexpression Increases Radiotherapy Response in HPV-Positive Head and Neck Cancer Through Inhibition of DNA Damage Repair and HPV E6 Downregulation

Elham Nafea Alsahafi[a,b] Selvam Thavaraj[c], Nazanin Sarvestani[a], Ofra Novoplansky[d], Moshe Elkabets[d], Bushra Ayaz[a] and Mahvash Tavassoli[a]*

Affiliations

[a]*Department of Molecular Oncology, Centre for Host Microbiome Interaction, King's College London, Guy's Hospital Campus, London SE1 1UL, UK*

[b]*Department of Basic and Clinical Sciences, Umm Al-Qura University, Faculty of Dentistry, Makkah 2373, Saudi Arabia*

[c]*Department of Head and Neck Pathology, Centre for Clinical, Oral and Translational Science, Guy's Hospital Campus, King's College London, SE1 9RT, UK*

[d]*The Shraga Segal Department of Microbiology, Immunology, and Genetics, Faculty of Health Sciences, Ben-Gurion University of the Negev, Beer-Sheva 84105, Israel*

***Corresponding author:** Professor Mahvash Tavassoli, Department of Molecular Oncology, King's College London, Hodgkin Building, London SE1 1UL, UK; Tel: +4420784896120; Email: mahvash.tavassoli@kcl.ac.uk*

Keywords: Head and Neck cancer; EGFR signalling; Human papillomavirus; Oropharyngeal squamous cell carcinoma (OPSCC); Radiation, DNA damage repair; HPV E6; P53; DNA double strand break

Abbreviations: HPV: human papillomavirus**,** HNSCC: head and neck squamous cell carcinoma, EGFR: Epidermal growth factor receptor, RT: radiotherapy, CT: chemotherapy, DDR: DNA damage repair, OPSCC: oropharyngeal squamous cell carcinoma, DSB: double strand break, HR: homologous recombination, NHEJ: non-homologous end joining, IR: ionising radiation, DNA-PKcs: DNA-dependent protein kinase, catalytic subunit, CRT: chemo-radiotherapy

Abstract

High-risk Human Papillomavirus (HPV) infections have recently emerged as an independent risk factor in head and neck squamous cell carcinoma (HNSCC). There has been a marked increase in the incidence of HPV-induced HNSCC subtype, which demonstrates different genetics with better treatment outcome. Despite the favourable prognosis of HPV-HNSCC, the treatment modality, consisting of high dose radiotherapy (RT) in combination with chemotherapy (CT), remains similar to HPV-negative tumours, associated with toxic side effects. Epidermal growth factor receptor (EGFR) is overexpressed in over 80% of HNSCC and correlates with RT resistance. EGFR inhibitor Cetuximab is the only FDA approved targeted therapy for both HNSCC subtypes, however the response varies between HNSCC subtypes. In HPV-negative HNSCC, Cetuximab sensitises HNSCC to RT improving survival rates. To reduce adverse cytotoxicity of CT, Cetuximab has been approved for treatment de-escalation of HPV-positive HNSCC. The results of several recent clinical trials have concluded differing outcome to HPV-negative HNSCC. Here we investigated the role of EGFR in HPV-positive HNSCC response to RT. Remarkably, in HPV-positive HNSCC cell lines, EGFR activation was strongly indicative of increased RT response in vitro and in vivo HNSCC tumour models. In response to RT, EGFR activation induced impairment of DNA damage repair and induced higher RT response. Furthermore, EGFR was found to downregulate HPV-E6 expression and induced p53 activity in response to RT. Collectively, our data uncovers a novel role for EGFR in virally induced HNSCC and highlights the importance of using EGFR-targeted therapies in the context of the genetic makeup of cancer.

Highlights

- EGFR activation is strongly correlated with worse survival outcome and radiotherapy resistance in HNSCC.
- HPV-positive HNSCC patients showed inferior outcomes when treated with Cetuximab, the only FDA-approved targeted agent for HNSCC.
- EGFR activation in HPV-positive HNSCC cell lines induced clear radiosensitisation in mice.
- EGFR overexpression resulted in inhibition of DNA damage repair as well as suppression of HPV-E6 oncoprotein, restoration of p53 activity and increased response to radiotherapy.
- EGFR function differs in virally derived HNSCC subtype, which needs to be considered before administration of EGFR targeted therapies to head and neck cancer patients.

1. Introduction

Head and neck squamous cell carcinomas (HNSCCs) are the sixth most common malignancy worldwide accounting for about 600,000 new cases annually, with poor 5-year overall survival rates [1]. There are two molecular subtypes determined by infection with human papillomavirus (HPV). HPV-negative tumours are biologically aggressive and driven by chemical mutagenesis linked to tobacco and alcohol use. The high mutational rate in key regulatory genes in HPV-negative tumours causes resistance to treatment and increased recurrence rate [2].

High-risk human papillomavirus is a causative agent for a subset of oropharyngeal squamous cell carcinoma and HPV16 accounts for over 90% of cases [3]. HPV-induced HNSCC arise specifically in the oropharynx (tonsils and base of the tongue) with incidence that has rapidly increased in recent years and has now exceeded the incidence of HPV-induced cervical cancer [4]. The viral oncoproteins E6 and E7 have the ability to inactivate the function of tumour suppressor proteins p53 and RB, respectively, which contribute largely to cell cycle deregulation and tumorigenesis [5]. Higher genomic instability, with lower mutational rate in oncogenes and tumour suppressors of HPV-induced tumours, creates a distinct molecular profile from HPV-negative tumours. Generally, HPV-induced HNSCC subtype respond better to standard therapies, radiotherapy (RT) alone or in combination with chemotherapy (CT) [6]. The molecular cause of increased sensitivity of HPV-positive HNSCC to RT/CT has not been comprehensively elucidated. Understanding the molecular mechanisms of increased sensitivity of HPV-positive HNSCC to therapy could generate information and potentially identify targetable pathways to improve treatment outcome of both HNSCC subtypes.

Epidermal growth factor receptor (EGFR) signalling pathway is vital for cellular proliferation, survival and metastasis. EGFR is overexpressed in 80-90% of HPV-negative HNSCCs and is associated with aggressive tumour behaviour and resistance to radio-chemotherapy [7, 8]. Radiotherapy has been the main treatment modality for HNSCC for decades but it is curative in only less than 50% of patients [9]. The underlying causes of response/resistance to RT are currently unknown but patients' genetics, epigenetics, metabolism, immune response and the microbiome, all have been implicated in RT response [10]. Radiotherapy induces double strand break (DSB), which is the most lethal form of DNA damage [11]. EGFR has been shown to directly and indirectly activating the repair of RT induced DSB through both homologous recombination (HR) and non-homologous end joining (NHEJ) mechanisms [12].

In response to ionising radiation (IR), EGFR becomes activated and translocates to the nucleus where it directly initiates transcription of DNA damage repair (DDR) genes [13]. Additionally, through activation of PI3K/AKT pathway EGFR initiates the recruitment and functioning of the DDR process [14]. Therefore, in response to IR, activated EGFR either translocates into the nucleus, where it binds to DNA-dependent protein kinase, catalytic subunit (DNA-PKcs) and regulatory subunit Ku70 to initiate DNA repair, or indirectly activates PI3K/AKT-dependent phosphorylation of DNA-PKcs resulting in enhanced DSB repair [15]. In 2006 Bonner et al, showed EGFR inhibition by monoclonal antibody Cetuximab, when used in combination with RT significantly increased HNSCC patient survival, and since then Cetuximab has been the only FDA approved targeted drug for the treatment of metastatic HNSCC [16]. Since 2017 immune checkpoint blockers have also been approved for the treatment of advanced HPV-positive and negative HNSCC, however so far only a very small percentage of patients have shown to benefit from targeted treatments [17].

As described above, HPV-positive HNSCC patients show better response to chemo-radiotherapy (CRT), and have in general better prognosis compared with HPV-negative HNSCC [18]. Hence, HPV is the only reliable molecular prognostic marker for HNSCC [19]. Despite distinctive clinical characteristics, there is currently no HNSCC subtype-specific treatment strategies available [20], both subtypes are treated with high dose RT/CT that is associated with severe cytotoxic side effects. This is particularly critical for the HPV-positive patients who are generally younger and likely to suffer long-term morbidities and experience reduced quality of life [21, 22]. In the absence of HPV specific treatment modalities, the major emphasis in recent years has been to de-intensify therapy protocols to reduce the toxic side effects, while maintaining the effective treatment [23]. To this end, several clinical trials have been conducted to replace chemotherapy with other forms of more specific treatments such as EGFR inhibitors (Table 1). However, the recent results of a major clinical trial, RTOG1016 concluded an unexpected but clear inferior survival in HPV-positive HNSCC patients who received Cetuximab in combination with RT as compared to patients who did not receive Cetuximab [24]. Similarly, the De-ESCALaTE clinical trial concluded that the substitution of Cisplatin with Cetuximab in HPV-positive HNSCC to be detrimental to disease control [23].

These clinical trials results question whether EGFR plays a true oncogenic role in HPV-positive as it clearly does in HPV-negative HNSCCs. To test this hypothesis, we investigated the role of EGFR signalling pathway in HPV-derived HNSCC cell lines and the effect of EGFR overexpression on RT response in HPV-positive HNSCC cell lines and mouse xenografts.

2. Materials and Methods

2.1 Cell lines and culture

The HNSCC cell lines SCC154, SCC090 (HPV-positive) and SCC072, SCC089 (HPV-negative) were a gift from Professor Susanne Gollin, University of Pittsburgh (Pittsburgh, PA, USA). UD-SCC2 (HPV-positive) was a gift from Professors H. Bier, University of Munich. HN5 (HPV-negative) was obtained from Professor Barry Gusterson, Department of Pathology, University of Glasgow, UK. HEK293T cells, which were used for retrovirus production, were a gift from Dr. Lucas Chan, Rayne Institute, King's College London, UK. The HEK293T, SCC089 and HN5 cells were maintained in Dulbecco's Modified Eagles Medium (DMEM; GE Healthcare, Chalfont St. Giles, UK) supplemented with 10% foetal bovine serum (FBS), 50-mg/ml streptomycin, 100-mg/ml penicillin and 1 mM sodium pyruvate. The HNSCC cell lines SCC154, SCC090, UD-SCC2 and SCC072 were cultured in MEM with Earle's salts supplemented with 10% FBS, 2 mM L-glutamine, 100µg/ml gentamicin and 1 × MEM non-essential amino acids. EGFR was stably overexpressed in selected HNSCC cell lines using retroviral vector as described previously [25]. The pBabe-puro control and EGFR overexpressing cells were selected using 2.5µg/ml puromycin. For treatment with recombinant EGF (Peprotech, London, UK), 500,000 cells per well were seeded in a 6-well plate. The next day, cells were serum-starved and 20-24hrs later treated with 100ng/ml recombinant EGF for the indicated time points.

2.2 Plasmids

The *pBabepuro* (control plasmid) is a retroviral mammalian expression vector containing LTR-promotor and *pBabepuro-EGFR* plasmid is a Human wild type EGFR cDNA cloned into Sal I site of pBabepuro, provided by Dr Paolo Di-Fiore, Department of Experimental Oncology, Institute Europeo di Oncologia, Milan, Italy.

2.3 Western blot analysis

Cells were lysed in lysis buffer (1 mM $MgCl_2$, 12.5 mM HEPES/KOH, pH 7.4, 1 mM EDTA, 1% Triton-X100) including protease inhibitors. Protein concentration was determined by Bradford assay, and 25 to 30µg of protein was separated on 8-15% 1.5mm thick SDS-gels and transferred to nitrocellulose membranes (350mA, 60min) using the Mini-PROTEAN electrophoresis system combined with the Mini-Trans Blot module (Bio-Rad, Hercules, CA, USA). Afterwards membranes were probed with the antibodies of choice. Antibodies used for immunoblotting were beta-actin, alpha-tubulin (Sigma-Aldrich, St. Louis, MO, USA), EGFR, phospho-ERK1/2, phospho-AKT (Ser473) phospho-EGFR (Tyr1068), phospho- STAT3 (Tyr705), Rad51, Ku80, DNA-PKcs (Cell signaling CST) and p53 (D-07) (Santa Cruz). Antibodies were used at a concentration of 1:1000 or 1:5000 (beta-actin, alpha-tubulin). Secondary HRP-coupled anti-rabbit (1:2000) and anti-mouse antibodies (1:2000) were

obtained from Fisher Scientific (Loughborough, UK) and Sigma-Aldrich (St. Louis, MO, USA), respectively.

2.4 Proliferation Assay

EGFR overexpressing and control cells were seeded in triplicate in 6-well plates (10,000 to 20,000 cells per well). Cells were harvested and counted in triplicate daily over 5 days. Proliferation was also assessed using the 3-(4,5-dimethylthiazol-2-yl)-2,5-diphenyltetrazolium bromide (MTT) cell viability assay as previously described [26]. Optical density was measured at a wavelength of 595nm on a Tecan Infinite F50.

2.5 Immunofluorescence

Cells were seeded at 15,000 to 30,000 cells per well in duplicate in 8-chamber slides (BD Biosciences, San Jose, CA, USA). The next day, cells were washed twice with 1X PBS and fixed in 4% paraformaldehyde for 15 min. Following 2 washing step with 1X PBS, cells were permeabilised for 15 min using 0.2% Triton-X100, then washed again and incubated for 30min in 3% bovine serum albumin (BSA) in TBS- Tween. Cells were incubated at 4 −C overnight under constant agitation in antibodies of choice (diluted in 3% BSA in TBS-Tween) or 3% BSA in TBS-Tween only as negative control. Afterwards, cells were washed twice using 1X PBS and then incubated with secondary fluorescently tagged antibody for 90min at 37C° protected from light. Following several washing steps in 1X PBS, the chambers were removed from the slides, and cells were mounted in Vectashield mounting medium containing 4,6-diamidin-2-phenylindole (DAPI; Vector Laboratories; Burlingame, CA, USA). Images were acquired in Nikon Centre (King's College London) at 60X or 100X magnifications. Antibodies used for immunofluorescence were EGFR, 53BP1 and gammaH2AX (Cell signaling CST).

2.6 ***Radiation Assays***

Radio-sensitivity of EGFR overexpressing cells and control cells were assessed using clonogenic assay as we have previously described [26]. Briefly, 3000 to 4000 cells were seeded in 6cm dishes and irradiated at different doses, dose 4Gy was chosen for further experiments, cells were incubated at 37°C for 7 to 14 days until colonies are formed. Colonies were fixed and stained with 6% glutaraldehyde and 1% crystal violet solution for 30min and counted.

2.7 Cell cycle analysis

Cell-cycle distribution was measured as previously described [27]. Cells were seeded in 3cm dishes and treated with either Gefitinib (Irressa) 2μM or IR (4Gy) or combination treatment. 24 hrs after treatments, cells were collected, fixed, treated with RNAse (Sigma, catalog # R-4875), stained with propidium iodide (PI), and read on FACS Canto II (Becton Dickinson, Oxford, UK). Data were analysed using Flowjo Software.

2.8 Neutral Comet Assay

DNA damage was assessed with a single-cell gel electrophoresis assay under neutral conditions. Briefly, cells were harvested at different time points after 4Gy γ-irradiation; mixed with low melting point agarose and plated on pre-coated (high melting point) agarose Comet Slide (Thermo Scientific, Cat no: 10393881). Cells were lysed overnight at 4°C, subjected to electrophoresis at 23V for 40min under neutral conditions, and stained with Ethidium Bromide (Sigma-Aldrich). Fifty cell nucleoids were assessed per slide, and each sample was analysed in triplicate using the Comet IV capture system (version 4.11; Perceptive Instruments, UK). The tail intensity (% tail DNA), defined as the percentage of DNA migrated from the head of the comet into the tail, was used as a measure of DNA damage induced [28].

2.9 Immunohistochemistry

Representative 5μm tissue sections from 10 separate cases of formalin fixed paraffin embedded normal and reactive tonsils were routinely prepared. EGFR extracellular domain immunohistochemical staining was undertaken using a prediluted proprietary kit (Clone 3C6, Roche Tissue Diagnostics) on a Ventana Benchmark Autostainer (Ventana Medical Systems) according to manufacturer's instructions. All samples were independently evaluated by at least two observers. An ordinate value of 0-3 was assigned to the intensity of staining. In each sample, scoring was allotted to surface epithelium and cryptal epithelium separately avoiding zones squamous metaplasia in the latter. The percentage of each intensity was allotted to full length of the surface and cryptal epithelium separately. A product of each intensity value and its percentage stained was determined. An 'H-Score' was then arrived at using the following formula: [(1X% cells intensity 1), (2X% cell intensity 2), (3X% cells intensity 3)]. The statistical difference between surface epithelium and cryptal epithelium H-scores was determined by un-paired t-test and data represented by box-and-whisker plot.

2.10 ***Patient tumour samples***

EGFR extracellular domain immunohistochemical staining was undertaken on representative whole-mount formalin-fixed paraffin embedded sections in 51 HPV-positive and 43 HPV-negative consecutive OPSCCs. HPV status was previously determined as part he diagnostic work up according to current national standards [29]. H-scores were evaluated as described above and the data represented as a dot over box-and-whisker plot. Statistical difference between HPV-positive and HPV-negative OPSCCs were determined using the Wilcoxon Signed Rank test. This part of the study was previously ethically approved (UK National Research Ethics Service (Reference: 10/H0701/27).

2.11 *Mice and in-vivo efficacy experiments*

NOD.Cg-Prkdc Il2rg/SzJ (NSG) mice were purchased from The Jackson Laboratory. Mice were maintained and treated in accordance with the institutional guidelines of Ben-Gurion University of the Negev. Animal experiments were approved by the Institutional Animal Care and Use Committee (IL.29-05-2018(E)). Mice were housed in air-filtered laminar flow cabinets with a 12-h light/dark cycle and food and water *ad libitum*. At the end of the experiment, animals were euthanised with CO_2. To obtain cell-line-derived xenografts 10×10^6 cells were injected subcutaneously into 6-week-old NSG mice. After about 20 days, when the tumour volume had reached 100 mm^3 the animals were randomly divided into groups, each group contained six mice harboring two tumours (n=12). Mice were anesthetised and a customised shielding was used to direct focal radiation to the tumour site. Three 6Gy fraction were given in alternating days. The dose rate was 1.33 Gy/minute. Tumours were measured with digital caliper, and tumour volumes were determined with the formula: length × $width^2 \times (\pi/6)$. Tumour volumes are plotted as means ± SEM. For immunohistochemistry, paraffin-embedded tumour blocks were sectioned at 5µm, loaded onto microscope slides, prepared as previously described [30] and stained for Ki67 (Cell marque corporation, Rocklin, CA, USA, 275R-14, 1:200). For fibrotic tissue Trichrome-Masson (Bio Optica, Milan, Italy, 04-01802) was used according to the manufacturer's instructions. All slides were digitalised using the Panoramic Scanner (3DHISTECH, Budapest, Hungary). Slides were analysed by QuantCenter (3DHISTECH) software.

2.12 Statistical analysis

Student's two-tailed t-test was performed for assessing differences between two independent groups. When measuring several independent factors between several groups, two-way ANOVA was used. The Wilcoxon Signed Rank test was used when assessing dependent variables. GraphPad Prism 8.2.1 was used for statistical analyses.

3. Results

3.1 Distinct EGFR expression level and subcellular localisation in HNSCC subtypes

In HNSCC, HPV infection is prevalent in the oropharyngeal mucosal regions and the tonsil represents the most commonly affected anatomical site [31]. The presence of highly specialised reticulated cryptal lymphoepithelium has been shown to be a favourable environment for HPV infection as the oral cavity and non-tonsillar areas in the oropharynx, lined by stratified squamous epithelium, serve as a barrier to HPV infection [32]. We therefore first evaluated EGFR protein expression in tonsillar epithelial tissues (surface and crypt) by IHC in 10 tissue samples of normal and reactive tonsils (Fig 1A). Surface epithelium consistently demonstrated higher EGFR level (mean total EGFR H score = 172) (Fig 1A a and c) compared to significantly lower EGFR level in reticulated cryptal epithelium (mean total EGFR H score =122.5) (Fig 1A b and d) and statistically significant ($p<0.001$, un-paired t-test) (Fig 1B). We then evaluated EGFR expression in patient tumour samples in correlation with HPV status (Fig 1C). The mean, mode, median and range for EGFR in HPV-positive tumours were 63, 45, 50 and 15-230, respectively (Fig 1C a and c). By contrast, the mean, mode, median and range for EGFR in HPV-negative tumours were 192, 190, 190 and 30-295, respectively (Fig 1C b and d). There was an overall trend for lower H-scores in HPV-positive HNSCC compared to HPV-negative tumours, ($p<0.001$, Wilcoxon Signed Rank Test) (Fig 1D).

To investigate the function of EGFR, a panel of HPV-positive and negative HNSCC cell lines were tested for EGFR expression, in general HPV-positive HNSCC cell lines have lower EGFR expression (Fig 1E), which is further confirmed by the analysis of TCGA dataset of EGFR expression in HNSCC subtypes (Fig 1F). We have previously shown that in general, HPV-positive HNSCC cell lines have similar sensitivity to various radiation doses (2, 4 and 6Gy) and demonstrated resistance to EGFR monoclonal antibody Cetuximab [33]. The low EGFR expressing HPV-positive SCC154 and low EGFR HPV-negative SCC072 cell lines were selected for overexpressing EGFR exogenously. Notably, SCC072 is derived from primary squamous cell carcinoma of tonsils (oropharynx) which is anatomically comparable to HPV-positive SCC154 cell line, while most other HPV-negative HNSCC cell lines available are derived from other sites which may not be a suitable comparison.

Successful modulation of EGFR was confirmed in both cell lines by Western blot analysis (Fig 1G and H). In HPV-negative SCC072, EGFR overexpression showed a 6-fold increase ($p<0.003$) (Fig 1G) compared to cells modulated with pBabe-puro (PBP) vector control. While in HPV-positive SCC154, EGFR overexpressing cells demonstrated a 6.2-fold increase ($p<0.002$) (Fig 1H) in total EGFR expression compared with PBP. The subcellular localisation of EGFR was also assessed by indirect immunofluorescence. EGFR overexpression in HPV-negative SCC072 resulted in a strong perinuclear staining with or without recombinant EGF stimulation compared to PBP control cells (Fig 1I) whereas

in HPV-positive SCC154 cells, EGFR overexpressing cells demonstrated mainly strong membranous EGFR staining both with and without recombinant EGF stimulation compared to control cells (Fig 1J).

3.2 EGFR regulates cellular proliferation, downstream signalling and cell cycle differently in two HNSCC subtypes

In HPV-negative SCC072 cells, EGFR overexpression increased proliferation rate compared to control cells by 2.2, 1.9 and 2.09-fold increase on day 3, 4 and 5, respectively (Fig 2A). By contrast, in HPV-positive SCC154 cells, EGFR overexpression significantly reduced cellular proliferation, by 1.7-fold on day 4 and 3.1-fold on day 5, respectively, compared to control cells (Fig 2B). Analysis of cell cycle profile of EGFR overexpressing and PBP controls revealed distinct cell cycle profile between HPV-negative and HPV-positive modulated cells. EGFR overexpression in HPV-negative SCC072 cells resulted in significant increase in G1 ($p<0.001$) and a small decrease in G2 phase of cell cycle (not statistically significant) compared to control cells (Fig 2C). By contrast, EGFR overexpression in HPV-positive SCC154 cells induced a significantly decreased G1 ($p<0.004$, Fig 2D) and increased G2 phase of cell cycle ($p<0.006$) (Fig 2D) in EGFR overexpressing cells compared to control cells.

Epithelial-mesenchymal transition (EMT) is a key feature allowing cancer cells to escape cellular stresses and metastasise to distant sites [34]. We evaluated the expression level of two major EMT markers: an epithelial marker (E-Cadherin) and a mesenchymal marker (Vimentin). In HPV-negative SCC072, EGFR overexpressing cells showed a significant increase in the mesenchymal marker Vimentin compared to PBP control (Fig S1A). Whereas HPV-positive SCC154 EGFR overexpressing cells demonstrated a marked increase in the epithelial marker E-cadherin, suggesting a role for EGFR in conferring an epithelial like phenotype in HPV-positive HNSCC cells (Fig S1A). Similar findings were confirmed by indirect immunofluorescence of E-cadherin and Vimentin expression in both HPV-negative and positive EGFR overexpressing cells (Fig S1B). Moreover, EGFR overexpression in HPV-negative SCC072 cells conferred oncogenic effects by demonstrating significant increased migration and invasive ability of EGFR overexpressing cells (Fig S2). As the consequence of EGFR overexpression was significantly different between HPV-negative and HPV-positive cells with regard to cellular proliferation and cell cycle profile, we investigated EGFR downstream signalling pathway in the absence/presence of recombinant EGF (100ng/ml). Without EGF stimulation, EGFR overexpression in both HPV-negative and HPV-positive cells showed increased EGFR tyrosine1068 phosphorylation (Fig 2E). In HPV-negative SCC072 cells, EGFR overexpression resulted in increased phosphorylation of STAT3, AKT serine437 and ERK1/2 compared to control cells (Fig 2E). Conversely, in HPV-positive SCC154 cells, EGFR overexpression induced a clear reduction in phosphorylation of STAT3, AKT serine473 and ERK1/2 (Fig 2E). Addition of EGF further induced

increased phosphorylation of AKT serine473 and ERK1/2 in HPV-negative SCC072 EGFR overexpressing compared to control cells but no change in STAT3 phosphorylation was observed (Fig 2E). By contrast, in HPV-positive SCC154 cells when EGFR overexpressing cells were stimulated with recombinant EGF (100ng/ml), a marked decrease in phosphorylation of AKT serine473 and pERK1/2 were observed as compared to control cells (Fig 2E). Interestingly, increased phosphorylation of STAT3 was observed in EGFR overexpressing HPV-positive cells compared to control (Fig 2E). Collectively, these results demonstrate a distinct role for EGFR in HPV-positive HNSCC, where excess EGFR signalling inhibits cell survival signalling pathway such as AKT and ERK1/2 resulting in the observed reduced proliferation and increased G2 cell cycle phase. The effects of EGFR on inhibition of cellular proliferation and reduced activity of AKT and ERK 1/2 were also confirmed in another HPV-positive HNSCC cell line SCC090 (Fig S3 D and F).

3.3 EGFR overexpression sensitises HPV-positive HNSCC cells to ionising radiation

A clear oncogenic role of EGFR in HPV-negative HNSCC has been established [35]. EGFR signalling is important to overcome radiation-induced DNA damage to ensure cell survival through EGFR-mediated activation of DNA repair proteins [36]. However, the impact of EGFR on response to DNA damage and repair in virally induced HNSCC is unclear. To investigate this function, EGFR overexpressing and control cells were irradiated at different doses of gamma radiation (2,4 and 6Gy) and a dose of 4Gy was found suitable for further studies. Cell survival was measured after 7-10 days when colonies were fixed and stained. The HPV-negative SCC072 EGFR overexpressing cells showed clear increased survival and radioresistance compared to control cells with statistically increased survival fraction (SF) at dose 4Gy ($p<0.04$) (Fig 3A and B). By contrast, HPV-positive SCC154 EGFR overexpressing cells demonstrated marked decrease in the number of surviving colonies and became radiosensitive compared to control cells with significant decreased SF at dose 4 and 6Gy ($p<0.01$ and $p< 0.02$) (Fig 3C and D). EGFR overexpressing and control cells were irradiated at a dose of 4Gy and stained for the presence of γ-H2AX foci within the nucleus as an established marker of double stranded DNA breaks [37]. The γ-H2AX foci rapidly accumulated and peaked at 30min after irradiation; foci remaining at 24hrs represents persistent damage suggesting increased radiosensitivity [38]. The HPV-negative SCC072 EGFR overexpressing cells demonstrated similar numbers of γ-H2AX foci per nucleus compared to control cells at 30min, however at 24hrs fewer foci were detected in EGFR overexpressing cells indicating more efficient repair in EGFR overexpressing cells (Fig 3E). Similarly, 30 min post radiation, the HPV-positive SCC154 EGFR overexpressing cells had similar numbers of γ-H2AX foci per nucleus compared to control. Remarkably, at 24hrs significantly higher number of foci were detected in EGFR overexpressing cells ($p<0.0005$) (Fig 3F) compared to control cells indicating persistent DNA damage caused by EGFR overexpression but only in HPV positive cells.

As EGFR is known to play an important role in IR-induced DNA DSB repair, we evaluated the expression of one of the major DSB repair proteins, 53-binding protein1 (53BP1) [39]. EGFR overexpressing and PBP control cells were irradiated at 4Gy and stained for 53BP1 foci at 1hr and 24hrs. The HPV-negative SCC072 EGFR overexpressing and control cells demonstrated similar number of 53BP1 foci at 1hr (Fig 3G). After 24hrs of IR-induced damage, EGFR overexpressing cells demonstrated increased ability in repairing DSB and demonstrated significant reduced 53BP1 foci compared to control cells ($p<0.01$) (Fig 3G). Whereas, HPV-positive SCC154 EGFR overexpressing cells contained significantly higher number of 53BP1 foci at 24hrs after IR suggesting EGFR-dependent reduced DSB repair (un-repaired DSB) ($p<0.0005$) (Fig 3H).

For further validation we studied IR-induced DNA DSB using the neutral comet assay, a single cell gel electrophoresis assay to detect relative amounts of DNA DSB [40]. HPV-negative SCC072 EGFR overexpressing cells demonstrated a lower percentage of DNA tail intensity at an early time point (30min) after IR-induced damage (Fig 3I) compared to control. However, at 24hrs the SCC072 EGFR overexpressing cells showed a significant resolution of DSB with decreased percentage of DNA tail intensity ($p<0.0011$) compared to control (Fig 3I). Remarkably, EGFR overexpression in HPV-positive SCC154 induced significant persistence of DSB in response to IR at early time point (30min) and increased percentage of DNA tail ($p<0.0071$) (Fig 3J) which increased further at 5hrs with significant increased percentage of DNA tail intensity ($p<0.0001$) compared to control c(Fig 3J). Notably, at 24hrs after IR, HPV-positive EGFR overexpressing cells demonstrated a significant delayed DSB repair and increased DNA tail intensity ($p<0.0001$) (Fig 3J).

Next, we tested whether the observed effects of EGFR overexpression were dependent on EGFR by using its specific TKI inhibitor Gefitinib. Cell cycle analysis demonstrated altered radioresistant phenotype in HPV-negative SCC072, when inhibiting EGFR with Gefitinib in combination with radiation (4Gy) (Fig 4A and B). A significant increase in sub G1 phase was observed in SCC072 EGFR overexpressing cells compared to treatment with radiation or Gefitinib alone (Fig 4C). Importantly, inhibition of EGFR activity by Gefitinib abrogated EGFR-induced radiosensitivity in HPV-positive SCC154 EGFR overexpressing cells by significantly reducing sub G1 ratio compared to treatment with radiation alone (Fig 4D and F). There was also a decrease in G2 phase in SSC154 EGFR overexpressing cells treated with Gefitinib in combination with radiation compared to treatment with radiation alone (Fig 4E). Collectively, the data supports that the effect of increased radiosensitivity and cell death in HPV-positive SCC154 EGFR overexpressing cells is EGFR-dependant.

Additionally, blocking EGFR in HPV-positive SCC154 using EGFR inhibitor AG1478 resulted in increased cell viability of EGFR overexpressing cells, supporting an EGFR-dependant effect of increased radiosensitivity in HPV-positive EGFR overexpressing cells (Fig S4).

3.4 EGFR overexpression in HPV-positive HNSCC cells reduces the efficiency of key DNA DSB repair proteins in response to ionising radiation

Radiotherapy induces DSB which is repaired by two major pathways; homologues recombination (HR) and non-homologues end joining (NHEJ) [11]. The repair of DSB during S phase or G2 phase is generally believed to involve HR, whereas, the NHEJ pathway is active throughout the cell cycle [41]. Impaired NHEJ pathway is believed to be important for radiosensitivity [42]. As demonstrated above, EGFR overexpression sensitised HPV-positive HNSCC to IR, with evidence that this is likely due to the impairment of the DSB repair process. We therefore investigated the effect of EGFR overexpression in both SCC072 and SCC154 cell lines on major DNA repair proteins after IR. Expression of RAD51, a marker of DSB repair through HR, was undetectable in the absence of IR-induced DNA damage in HPV-negative SCC072 EGFR overexpressing and control cells (Fig 5A and B). However, after IR, EGFR overexpressing cells showed significant increase in RAD51 protein level as early as 30min ($p<0.0116$) (Fig 5A and B) that persisted until 5hrs post-radiation ($p<0.0446$) (Fig 5A and B).

Conversely, HPV-positive SCC154 EGFR overexpressing cells showed slight decreased RAD51 protein level in the absence of IR-induced DNA damage compared to control ($p<0.113$) (Fig 5C and D). Importantly, in response to IR-induced DSB, EGFR overexpressing SCC154 cells showed significant decrease in the level of RAD51 protein at 30min, 2 and 5hrs ($p<0.001$, $p<0.001$ and $p<0.048$ respectively) (Fig 5C and D). These results clearly indicate that EGFR plays important but distinct roles in HPV-positive cells and delays the repair of DSB sensitising cancer cells to IR.

The influence of EGFR overexpression on some NHEJ repair proteins was also assessed; Ku80 is a key member of NHEJ pathway and serves as a docking station for co-factors involved in DSB repair [43]. The HPV-negative SCC072 EGFR overexpressing cells showed a higher level of Ku80 protein in the absence of IR-induced DNA damage compared to control ($p<0.0021$) (Fig 5A and B). In response to IR the EGFR overexpressing cells demonstrated a significant increase in Ku80 protein level at 30min that persisted at 2hrs post-radiation ($p<0.042$ and $p<0.049$, respectively) compared to control (Fig 5A and B). By contrast, HPV-positive SCC154 EGFR overexpressing cells showed significant reduction in Ku80 levels at 30min and 5hrs post-radiation ($p<0.025$ and $p<0.048$, respectively) compared to control (Fig 5C and D).

The level of DNA-PKcs, a repair protein directly activated by EGFR signalling was also investigated. EGFR overexpression in HPV-negative SCC072 showed significant increase in the activity of DNA-PKcs in the absence of IR ($p<0.047$) (Fig 5E and F). The increase in DNA-PKcs activity continued in the presence of IR-induced damage at 30min ($p<0.001$) and 5hrs ($p<0.001$) accompanied by a

significant increased phosphorylation of AKT Ser473 at 30min ($p<0.001$), 2hrs ($p<0.03$) and 5hrs ($p<0.01$) (Fig 5E and F). Conversely, The HPV-positive SCC154 EGFR overexpressing cells demonstrated a significantly reduced level of DNA-PKcs at 30min post IR ($p<0.004$) (Fig 5G and H) that persisted until 5hrs post-radiation ($p<0.010$) (Fig 5G and H) compared to control. The reduction in DNA-PKcs activity was associated with a significantly reduced p-AKT Ser473 in EGFR overexpressing cells in response to IR at 30min ($p<0.007$), 2hrs (0.005) and 5hrs (0.001) (Fig 5G and H). Together, the data shows that EGFR overexpression enhances the repair of IR-induced DSB in HPV-negative SCC072 by activating major DDR proteins including RAD51, Ku80 and DNA-PKcs through HR and NHEJ pathways. By contrast in HPV-positive SCC154, EGFR overexpression has the completely opposite role and delays the resolution of IR-induced DSBs by reducing the expression of key repair proteins. Markedly, the increased radiosensitivity and decreased survival caused by EGFR overexpression was specific to IR-induced DNA double strand break as the response of HPV-negative and HPV-positive cells to chemotherapeutic drug Cisplatin was not influenced by EGFR overexpression (Fig S5).

3.5 EGFR overexpression in HPV-positive HNSCC cells downregulates HPV-E6, inducing p53 re-activation in response to ionising radiation

The TP53 tumour suppressor has a central role in regulating response to cellular stress such as IR-induced damage [44]. Given that HPV infected cells in general retain a wild type p53 which is degraded by E6-AP, but could be re-activated, we investigated the p53 activation in HPV-positive SCC154 EGFR overexpressing and control cells in response to IR. EGFR overexpression resulted in a clear increase in p53 level in SCC154 cells (Fig 5I). Furthermore, in response to IR at 4Gy, the HPV-positive SCC154 EGFR overexpressing cells demonstrated increased level of p53 compared to control (Fig 5I) as well as an increase in the p53 target $p21^{cip1/waf1}$ (Fig 5I) indicating EGFR-mediated functional activity of p53 in HPV positive HNSCC cells.

In HPV-positive SCC154 cell line, wild type p53 is depleted through E6-dependent proteasomal degradation, we therefore investigated whether EGFR overexpression had any effect on the expression of HPV-E6 by qRT-PCR. Remarkably, EGFR overexpression in HPV-positive SCC154 induced an approximately 80% reduction in E6 expression level compared to control ($p>0.001$) (Fig 5J). This effect was also observed in another independent HPV-positive HNSCC cell line SCC090 (Fig. S3 F). These results identify a novel function for EGFR in HPV-positive HNSCC cells in abrogating the expression of HPV16 E6 leading to re-activation of p53. Consequently, EGFR mediated inhibition of E6 and re-activation of p53 induces G2 arrest, delayed DSB resolution leading to increased radio-sensitivity.

3.6 EGFR overexpression in HPV-positive SCC154 increases radiosensitivity in *in-vivo* model

To validate the results of *in-vitro* increased radiosensitivity study of HPV-positive SCC154 EGFR overexpressing cells, we explored the effects of EGFR overexpression on the response to radiation in *in-vivo* using the tumourigenic HPV-positive SCC154 xenograft model. EGFR overexpressing and control (PBP) cells were injected subcutaneously into NSG mice. Similar to *in-vitro* results, EGFR overexpressing xenograft tumours demonstrated slower growth rate compared to controls (154 PBP) (Fig S6). Radiation was administered to the treated group when tumours reached the size of $100mm^3$. In 154 PBP tumour group, radiation treatment had a minimal effect on tumour growth (Fig 6A). Conversely, the EGFR overexpressing (154 EGFR) tumours were significantly sensitive to radiation, as indicated by delayed tumour growth at day 6 and 8 ($p<0.03$ and $p<0.001$) (Fig 6B). Remarkably, the histopathology of EGFR overexpressing tumours showed a significant reduction in the number of proliferated tumour cells in irradiated group compared to controls, indicated by Ki76 positive staining ($p<0.0001$) (Fig 6C). Furthermore, the irradiated EGFR overexpressing xenograft tumours showed an increase in radiation-induced collagen-rich fibrotic tissue as demonstrated by Trichrome-Masson staining, when compared to control group ($p<p<0.0001$) (Fig 6D).

4. Discussion

The current standard of care for locally advanced HNSCCs does not differentiate between HPV-negative and HPV-positive tumours, both subtypes are treated similarly with highly toxic chemo-radiotherapy [45]. This is despite the well-established understanding of HPV-induced HNSCC representing a different subtype, generally affecting younger patients and having favourable treatment outcomes [46]. The aggressive treatment regimens for HPV-induced tumours has demanded a shift toward less-toxic, targeted de-intensified regimes, which has driven a number of clinical trials [47].

EGFR overexpression has been an established biomarker associated with decreased survival, increased distant metastasis and treatment resistance in HPV-negative HNSCC [35]. However, a clear role for EGFR in relation to prognosis and therapy outcomes in HPV-positive HNSCC has not so far been established [48] [49].

To understand the role of EGFR in HPV-positive HNSCC, we first established the consistent low EGFR expression in reticulated cryptal tonsil epithelium, easily-exposed and preferable site for HPV infections [50]. Low EGFR expression in cryptal tonsil epithelium may be advantageous for HPV infection and

persistence. This notion is clearly supported by our data of consistent low EGFR expression in HPV-positive HNSCC tumour samples and cell lines (Fig 1C, D, E and F). Our findings that EGFR overexpression caused significant decrease in the expression of HPV-E6 and reactivated p53 (Fig 5I and J) provides further evidence of a role for EGFR in modulating the process of HPV infection and/or its oncogenic function.

Our data reinforced a clear oncogenic activity for EGFR in HPV-negative HNSCC cells conferring increased survival, EMT and radiotherapy resistance. We also demonstrated a nuclear/perinuclear EGFR localisation specifically in HPV-negative HNSCC. In several cancer types including HNSCC nuclear EGFR has been implicated in therapy resistance through several mechanisms, including acting as a transcription factor, binding and enhancing activities of oncogenes such as cyclin D1, iNOS, B-Myb and COX-2 genes [51]. Additionally, nuclear EGFR has shown to activate DNA damage repair pathways to resolve treatment induced DNA damage thereby maintaining cell survival [52]. Nuclear EGFR has been shown to stabilise PCNA increasing chromatin stability and cell survival [12]. Furthermore, nuclear EGFR has been shown to induce radioresistance by directly interacting and phosphorylating DNA-PKcs activating DBS repair [53]. Alternatively, EGFR cellular signalling through activation of downstream PI3K/AKT pathway leads to the repair of radiotherapy induced DSB escaping cell death [15, 36, 54, 55]. The specific roles of nuclear versus membranous EGFR were not studied here and require further investigation.

Here we found EGFR overexpression in HPV-negative HNSCC cells to induce a clear radioresistance phenotype by activating the main DSB repair proteins resolving IR-induced DNA damage and increasing cell survival. By contrast, in HPV-positive HNSCC, EGFR overexpression significantly increased radiosensitivity by downregulating the expression of the main repair proteins of both HR and NHEJ pathways, impairing resolution of IR-induced DSB and inducing cell death. Importantly, these effects were EGFR dependent as commonly used EGFR TKI Gefitinib and another selective EGFR inhibitor AG1478 abrogated these effects. These findings are in agreement with several preclinical studies demonstrating blocking EGFR activation in HPV-negative HNSCC tumours inhibits the repair of IR-induced DNA damage increasing radiosensitivity of HNSCC tumour models [54, 56]. Furthermore, we confirmed the effect of EGFR overexpression on response to radiation using *in-vivo* xenograft model by demonstrating delayed tumour growth, tumour volume and increased fibrosis in EGFR overexpressing xenograft tumours, supporting the *in-vitro* observation of increased radiosensitivity in HPV-positive EGFR overexpressing cells. Remarkably, the significant increase of radiation-induced collagen-fibrotic tissues in EGFR overexpressing xenograft tissues suggested a role of EGFR overexpression in increased tumour fibrosis and slower tumour growth that potentially could create a barrier against tumour cell metastasis. This interesting observation has been reported in

fibrosarcoma tissues, where increased radiation-induced collagen shown to inhibit tumour growth and metastasis [57]. We found EGFR inhibition in the HPV-positive HNSCC cells to decrease IR-induced cell death, further supporting a radiosensitisation role for EGFR in the HPV induced HNSCC cells.

The exact mechanism of EGFR-induced radiosensitisation in HPV-positive HNSCC tumours remains unclear. Ideally, normal keratinocytes should be included in experiments investigating radiosensitivity of HNSCC cell lines, which is generally lacking and has only been used in few studies [58]. This is mainly due to the short lifespan of normal keratinocytes and the difficulty in modulating and carrying out long term treatment experiments such as clonogenicity. As discussed above, EGFR overexpression resulted in a clear reduction in the activity of DNA damage repair proteins and increased G2 in HPV-positive but not HPV-negative HNSCC cells. TP53 is the main regulator of G2 arrest during which the fate of the cell is decided by the ability of DDR machinery to either repair, and continue through the cell cycle, or induce cell death due to excess unrepaired DNA damage [59]. TP53 is mutated in around 85% of HPV-negative HNSCC cases and is believed to be one of the main resistance mechanisms to standard therapy [60]. The p53 protein is inactivated in HPV-induced tumours through degradation by HPV-E6 oncoprotein. Unlike mutant p53 the activity of wild type p53 in HPV-positive cancers can be restored under certain condition in response to DNA damage, and reactivation of p53 has been suggested as one of mechanisms causing increased radiosensitivity of HPV-positive HNSCC [61].

We found EGFR overexpression in HPV-positive cells to reduce ERK1/2 and AKT activation, pathways vital for cellular proliferation and survival (Fig 2G). Additionally, these effects were reproduced in EGFR overexpressing xenograft tumours tissues which, demonstrated significant reduced proliferation in response to radiation (Fig 6C). EGFR overexpression in HPV-positive HNSCC cells resulted in stabilisation of wild-type p53 and induction of its target p21 tumour suppressor inducing a G2 arrest and subsequent cell death (Fig 5I). Moreover, EGFR overexpression in HPV-positive HNSCC cells significantly reduced the expression of HPV16 E6 in two independent HPV-positive cell lines (Fig 5J and Fig S3 F). These results which to our knowledge have not been reported previously, allude to a possible mechanism of EGFR-induced reactivation of p53 and p21, prolonged G2 arrest, inactivation of DSB repair and consequently induction of cell death in response to IR.

The observation of downregulation of E6 by EGFR is interesting but the actual mechanism currently remains unclear. In one report excessive EGFR signalling was shown to shorten the lifespan of normal human keratinocytes (HKs) and demonstrated the failure of forced E6 expression in HKs that had high EGFR basal level, indicating a function for EGFR in preventing E6 expression [62]. Tentatively, EGFR-induced downregulation of oncoprotein E6 expression could be regulated by microRNAs or long non-coding RNAs (lncRNAs). EGFR has been shown to interfere and regulate microRNAs biogenesis via binding to AGO2, a critical component of RISC complex responsible for microRNAs biogenesis

[63]. Moreover, host microRNAs can regulate expression of high-risk HPV viral proteins [64]. However, we have currently no evidence of any physical or functional interaction of HPV-EGFR-microRNA axis, which will be investigated in future studies. Alternatively, telomeres dysfunction has been shown to regulate radiosensitivity in HNSCC cells [65] and HPV E6 is known to directly regulate telomere function [66-68]. Thus, whether the increased radiosensitivity in HPV-positive EGFR overexpressing cells is partly attributed to telomere dysfunction remains to be investigated.

Several studies investigating EGFR expression and HPV status in HNSCC have reported an inverse correlation [4, 69]. In one study the prognostic value of HPV status and phosphorylated EGFR protein (p-EGFR Tyr1068) by immunohistochemistry was investigated and showed better overall survival and 5-years disease free progression associated with increased p-EGFR Tyr1068 activity when compared to HPV-positive, p-EGFR negative expression cohort [48]. This finding agrees with our data demonstrating a link between increased phosphorylated levels of EGFR Tyr1068 with better response to IR in HPV-positive SCC154 cells. With respect to de-escalating treatment strategies for HPV-derived tumours, several studies have investigated DDR targeted drugs [70]. Inhibitors of poly (ADP-ribose)-polymerases (PARP) in HPV-positive HNSCC cells were found to increases responsiveness to IR. As a well-tolerated agent, PARP targeted drugs were found to be more effective than EGFR inhibitor Cetuximab in a panel of HPV-positive HNSCC cell lines, including SCC154 cell line, which showed increased radiosensitivity [71]. Collectively, the analysis of DDR pathway in HNSCC cell lines identified distinct roles for EGFR in regulating DNA repair and RT response. To our knowledge this is the first report of EGFR playing a potential role in increasing radiosensitivity specifically in virally induced HNSCC, and could provide a possible answers to the surprising outcome of several recent clinical trials concluding giving EGFR inhibitor Cetuximab to HPV-positive HNSCC patients is significantly inferior [23, 24]. Therefore, this data highlights the need for better understanding of this major signalling pathway in HPV-positive HNSCC and questions its therapeutic benefit in certain types of cancers [18, 49].

5. Conclusion

This study findings propose a novel function of EGFR in HPV-positive HNSCC cells, where EGFR overexpression results in reduced AKT activity causing and increased radiosensitisation mainly through impairment of IR-induced DSB repair through non-homologous end joining (NHEJ) repair pathways. Moreover, a novel role of EGFR in suppressing HPV-16 E6 expression and increased functional p53 was identified, although the exact mechanism is yet to be established in future studies (Fig 7). Understanding the mechanisms of inherent radiosensitivity of HPV-derived tumours will help in

implementing effective and less toxic tailored therapy for each specific HNSCC subtype. The translational aspect of our findings is dependent on identifying the mechanisms by which EGFR is regulating radiosensitivity in HPV-derived HNSCC cells including potential mechanisms through modulation of tumour microenvironment via exosomes, transcriptional regulation of E6 through microRNAs and identifying alternative targets regulated by EGFR. We believe, our findings make an important contribution towards unravelling the complexity of varying response of HNSCC patients to radiotherapy. These findings identify an alternative radiosensitising role for EGFR in HPV-induced HNSCC. Exploring the mechanisms by which EGFR downregulates HPV-E6 expression and abrogates its function would provide a new insight into the molecular pathogenesis of HPV-induced cancers.

Acknowledgement

The authors would like to thank Dr Volker Arlt and Dr Halh Al-Serori from MRC-PHE Centre for Environment & Health, King's College London for help in performing Comet assay. Katheryn Begg for helping with radiation experiments. Dr Marcos Jose Custodio Neto Da Silva for helping with HPV-E6 experiments. Leonid Olender, for helping with in-vivo xenograft model's radiation experiments. Elham Nafea Alsahafi is funded by a scholarship from Umm Al-Qura University, Faculty of Dentistry, Makkah City, Saudi Arabia. Grant/Award Number: 4350157921. Ofra Novoplasnky was supported by the Eileen & Louis Dubrovsky Doctoral/Post-Doctoral Cancer Fellowship. We would like to thank the Rosetrees Trust and Stoneygate Trust for supporting part of this study through grant reference M117-F2 to M.T and the Israeli Cancer Research Foundation (ICRF, 17-1693-RCDA to M.E)

Conflict of interest statement

Non declared for all authors.

References

[1] C.R. Leemans, P.J.F. Snijders, R.H. Brakenhoff, The molecular landscape of head and neck cancer, Nat Rev Cancer, 18 (2018) 269-282.

[2] B. Solomon, R.J. Young, D. Rischin, Head and neck squamous cell carcinoma: Genomics and emerging biomarkers for immunomodulatory cancer treatments, Semin Cancer Biol, (2018).

[3] M. Taberna, M. Mena, M.A. Pavon, L. Alemany, M.L. Gillison, R. Mesia, Human papillomavirus-related oropharyngeal cancer, Ann Oncol, 28 (2017) 2386-2398.

[4] S. Thavaraj, A. Stokes, K. Mazuno, R. Henley-Smith, Y.E. Suh, V. Paleri, M. Tavassoli, E. Odell, M. Robinson, Patients with HPV-related tonsil squamous cell carcinoma rarely harbour oncogenic HPV infection at other pharyngeal sites, Oral Oncol, 50 (2014) 241-246.

[5] D. Sano, N. Oridate, The molecular mechanism of human papillomavirus-induced carcinogenesis in head and neck squamous cell carcinoma, Int J Clin Oncol, 21 (2016) 819-826.

[6] R.H. Brakenhoff, S. Wagner, J.P. Klussmann, Molecular Patterns and Biology of HPV-Associated HNSCC, Recent Results Cancer Res, 206 (2017) 37-56.

[7] R.B. Cohen, Current challenges and clinical investigations of epidermal growth factor receptor (EGFR)- and ErbB family-targeted agents in the treatment of head and neck squamous cell carcinoma (HNSCC), Cancer Treat Rev, 40 (2014) 567-577.

[8] S. Sigismund, D. Avanzato, L. Lanzetti, Emerging functions of the EGFR in cancer, Molecular oncology, 12 (2018) 3-20.

[9] W.M. Mendenhall, R. Dagan, C.M. Bryant, R.P. Fernandes, Radiation Oncology for Head and Neck Cancer: Current Standards and Future Changes, Oral Maxillofac Surg Clin North Am, 31 (2019) 31-38.

[10] E. Alsahafi, K. Begg, I. Amelio, N. Raulf, P. Lucarelli, T. Sauter, M. Tavassoli, Clinical update on head and neck cancer: molecular biology and ongoing challenges, Cell Death Dis, 10 (2019) 540.

[11] M.E. Lomax, L.K. Folkes, P. O'Neill, Biological consequences of radiation-induced DNA damage: relevance to radiotherapy, Clin Oncol (R Coll Radiol), 25 (2013) 578-585.

[12] G. Liccardi, J.A. Hartley, D. Hochhauser, EGFR nuclear translocation modulates DNA repair following cisplatin and ionizing radiation treatment, Cancer Res, 71 (2011) 1103-1114.

[13] T.M. Brand, M. Iida, N. Luthar, M.M. Starr, E.J. Huppert, D.L. Wheeler, Nuclear EGFR as a molecular target in cancer, Radiother Oncol, 108 (2013) 370-377.

[14] D. Horn, J. Hess, K. Freier, J. Hoffmann, C. Freudlsperger, Targeting EGFR-PI3K-AKT-mTOR signaling enhances radiosensitivity in head and neck squamous cell carcinoma, Expert Opinion on Therapeutic Targets, 19 (2015) 795-805.

[15] Z. Zhou, H. Lu, S. Zhu, A. Gomaa, Z. Chen, J. Yan, K. Washington, W. El-Rifai, C. Dang, D. Peng, Activation of EGFR-DNA-PKcs pathway by IGFBP2 protects esophageal adenocarcinoma cells from acidic bile salts-induced DNA damage, Journal of experimental & clinical cancer research : CR, 38 (2019) 13.

[16] J.A. Bonner, P.M. Harari, J. Giralt, N. Azarnia, D.M. Shin, R.B. Cohen, C.U. Jones, R. Sur, D. Raben, J. Jassem, R. Ove, M.S. Kies, J. Baselga, H. Youssoufian, N. Amellal, E.K. Rowinsky,

K.K. Ang, Radiotherapy plus cetuximab for squamous-cell carcinoma of the head and neck, N Engl J Med, 354 (2006) 567-578.

[17] M.D. Forster, M.J. Devlin, Immune Checkpoint Inhibition in Head and Neck Cancer, Frontiers in oncology, 8 (2018).

[18] C. Liu, D. Mann, U.K. Sinha, N.C. Kokot, The molecular mechanisms of increased radiosensitivity of HPV-positive oropharyngeal squamous cell carcinoma (OPSCC): an extensive review, J Otolaryngol Head Neck Surg, 47 (2018) 59.

[19] R.J. Kimple, P.M. Harari, The prognostic value of HPV in head and neck cancer patients undergoing postoperative chemoradiotherapy, Annals of translational medicine2015.

[20] A.G. Sacco, F.P. Worden, Molecularly targeted therapy for the treatment of head and neck cancer: a review of the ErbB family inhibitors, Onco Targets Ther, 9 (2016) 1927-1943.

[21] M. Machtay, J. Moughan, A. Trotti, A.S. Garden, R.S. Weber, J.S. Cooper, A. Forastiere, K.K. Ang, Factors associated with severe late toxicity after concurrent chemoradiation for locally advanced head and neck cancer: an RTOG analysis, J Clin Oncol, 26 (2008) 3582-3589.

[22] H. Abed, D. Reilly, M. Burke, B. Daly, Patients with head and neck cancers' oral health knowledge, oral health-related quality of life, oral health status, and adherence to advice on discharge to primary dental care: A prospective observational study, Spec Care Dentist, 39 (2019) 593-602.

[23] H. Mehanna, M. Robinson, A. Hartley, A. Kong, B. Foran, T. Fulton-Lieuw, M. Dalby, P. Mistry, M. Sen, L. O'Toole, H. Al Booz, K. Dyker, R. Moleron, S. Whitaker, S. Brennan, A. Cook, M. Griffin, E. Aynsley, M. Rolles, E. De Winton, A. Chan, D. Srinivasan, I. Nixon, J. Grumett, C.R. Leemans, J. Buter, J. Henderson, K. Harrington, C. McConkey, A. Gray, J. Dunn, Radiotherapy plus cisplatin or cetuximab in low-risk human papillomavirus-positive oropharyngeal cancer (De-ESCALaTE HPV): an open-label randomised controlled phase 3 trial, Lancet, 393 (2019) 51-60.

[24] M.L. Gillison, A.M. Trotti, J. Harris, A. Eisbruch, P.M. Harari, D.J. Adelstein, E.M. Sturgis, B. Burtness, J.A. Ridge, J. Ringash, J. Galvin, M. Yao, S.A. Koyfman, D.M. Blakaj, M.A. Razaq, A.D. Colevas, J.J. Beitler, C.U. Jones, N.E. Dunlap, S.A. Seaward, S. Spencer, T.J. Galloway, J. Phan, J.J. Dignam, Q.T. Le, Radiotherapy plus cetuximab or cisplatin in human papillomavirus-positive oropharyngeal cancer (NRG Oncology RTOG 1016): a randomised, multicentre, non-inferiority trial, Lancet, 393 (2019) 40-50.

[25] M. Flinterman, J. Gaken, F. Farzaneh, M. Tavassoli, E1A-mediated suppression of EGFR expression and induction of apoptosis in head and neck squamous carcinoma cell lines, Oncogene, 22 (2003) 1965-1977.

[26] Y.E. Suh, N. Raulf, J. Gaken, K. Lawler, T.G. Urbano, J. Bullenkamp, S. Gobeil, J. Huot, E. Odell, M. Tavassoli, MicroRNA-196a promotes an oncogenic effect in head and neck

771 cancer cells by suppressing annexin A1 and enhancing radioresistance, Int J Cancer, 137
772 (2015) 1021-1034.

773 [27] H.M. Hersi, N. Raulf, J. Gaken, N. Folarin, M. Tavassoli, MicroRNA-9 inhibits growth
774 and invasion of head and neck cancer cells and is a predictive biomarker of response to
775 plerixafor, an inhibitor of its target CXCR4, Molecular oncology, 12 (2018) 2023-2041.

776 [28] S. Imanikia, F. Galea, E. Nagy, D.H. Phillips, S.R. Sturzenbaum, V.M. Arlt, The
777 application of the comet assay to assess the genotoxicity of environmental pollutants in
778 the nematode Caenorhabditis elegans, Environ Toxicol Pharmacol, 45 (2016) 356-361.

779 [29] National Institute of Health and Care Excellance, Cancer of the upperaerodigestive
780 tract: assessment and management in people aged 16 and over, 2018.

781 [30] K.M. Yegodayev, O. Novoplansky, A. Golden, M. Prasad, L. Levin, S. Jagadeeshan, J.
782 Zorea, O. Dimitstein, B.-Z. Joshua, L. Cohen, E. Khrameeva, M. Elkabets, TGF-Beta-
783 Activated Cancer-Associated Fibroblasts Limit Cetuximab Efficacy in Preclinical Models
784 of Head and Neck Cancer, Cancers, 12 (2020) 339.

785 [31] M. Wojtera, J. Paradis, M. Husein, A.C. Nichols, J.W. Barrett, M.I. Salvadori, J.E.
786 Strychowsky, The prevalence of human papillomavirus in pediatric tonsils: a systematic
787 review of the literature, Journal of otolaryngology - head & neck surgery = Le Journal
788 d'oto-rhino-laryngologie et de chirurgie cervico-faciale, 47 (2018) 8.

789 [32] R.S.R. Woods, H. Keegan, C. White, P. Tewari, M. Toner, S. Kennedy, E.M. O'Regan, C.M.
790 Martin, C.V.I. Timon, J.J. O'Leary, Cytokeratin 7 in Oropharyngeal Squamous Cell
791 Carcinoma: A Junctional Biomarker for Human Papillomavirus-Related Tumors, Cancer
792 Epidemiol Biomarkers Prev, 26 (2017) 702-710.

793 [33] B. Ayaz, Human Papillomavirus-mediated Response of Head and Neck Cancer Cells
794 to Therapeutic Agents, King's College London, PhD thesis, 2016.

795 [34] T. Fujiwara, T. Eguchi, C. Sogawa, K. Ono, J. Murakami, S. Ibaragi, J.I. Asaumi, S.K.
796 Calderwood, K. Okamoto, K.I. Kozaki, Carcinogenic epithelial-mesenchymal transition
797 initiated by oral cancer exosomes is inhibited by anti-EGFR antibody cetuximab, Oral
798 Oncol, 86 (2018) 251-257.

799 [35] P. Bossi, C. Resteghini, N. Paielli, L. Licitra, S. Pilotti, F. Perrone, Prognostic and
800 predictive value of EGFR in head and neck squamous cell carcinoma, Oncotarget, 7 (2016)
801 74362-74379.

802 [36] M. Toulany, H.P. Rodemann, Phosphatidylinositol 3-kinase/Akt signaling as a key
803 mediator of tumor cell responsiveness to radiation, Semin Cancer Biol, 35 (2015) 180-
804 190.

805 [37] A. Sharma, K. Singh, A. Almasan, Histone H2AX phosphorylation: a marker for DNA
806 damage, Methods in molecular biology (Clifton, N.J.), 920 (2012) 613-626.

[38] D. Klokov, S.M. MacPhail, J.P. Banath, J.P. Byrne, P.L. Olive, Phosphorylated histone H2AX in relation to cell survival in tumor cells and xenografts exposed to single and fractionated doses of X-rays, Radiotherapy and oncology : journal of the European Society for Therapeutic Radiology and Oncology, 80 (2006) 223-229.

[39] B. Cirauqui, M. Margeli, V. Quiroga, A. Quer, N. Karachaliou, I. Chaib, J.L. Ramirez, A. Munoz, C. Pollan, I. Planas, A. Drozdowsky, R. Rosell, DNA repair pathways to regulate response to chemoradiotherapy in patients with locally advanced head and neck cancer, Tumour biology : the journal of the International Society for Oncodevelopmental Biology and Medicine, 37 (2016) 13435-13443.

[40] J. Zhao, Z. Guo, H. Zhang, Z. Wang, L. Song, J. Ma, S. Pei, C. Wang, The potential value of the neutral comet assay and γH2AX foci assay in assessing the radiosensitivity of carbon beam in human tumor cell lines, Radiology and oncology, 47 (2013) 247-257.

[41] A. Kakarougkas, P. Jeggo, DNA DSB repair pathway choice: an orchestrated handover mechanism, The British journal of radiology, 87 (2014) 20130685.

[42] S.A. Bhide, K. Thway, J. Lee, K. Wong, P. Clarke, K.L. Newbold, C.M. Nutting, K.J. Harrington, Delayed DNA double-strand break repair following platin-based chemotherapy predicts treatment response in head and neck squamous cell carcinoma, British journal of cancer2016, pp. 825-830.

[43] B.B. Kragelund, E. Weterings, R. Hartmann-Petersen, G. Keijzers, The Ku70/80 ring in Non-Homologous End-Joining: easy to slip on, hard to remove, Front Biosci (Landmark Ed), 21 (2016) 514-527.

[44] R. Kang, G. Kroemer, D. Tang, The tumor suppressor protein p53 and the ferroptosis network, Free radical biology & medicine, (2018).

[45] P. Kozakiewicz, L. Grzybowska-Szatkowska, Application of molecular targeted therapies in the treatment of head and neck squamous cell carcinoma, Oncol Lett, 15 (2018) 7497-7505.

[46] M. Wierzbicka, K. Szyfter, P. Milecki, K. Skladowski, R. Ramlau, The rationale for HPV-related oropharyngeal cancer de-escalation treatment strategies, Contemp Oncol (Pozn), 19 (2015) 313-322.

[47] Determination of Cetuximab Versus Cisplatin Early and Late Toxicity Events in HPV+ OPSCC - Full Text View - ClinicalTrials.gov, (2018).

[48] M. Taberna, M. Torres, M. Alejo, M. Mena, S. Tous, S. Marquez, M.A. Pavon, X. Leon, J. Garcia, M. Guix, R. Hijano, T. Bonfill, A. Aguila, A. Lozano, R. Mesia, L. Alemany, I.G. Bravo, The Use of HPV16-E5, EGFR, and pEGFR as Prognostic Biomarkers for Oropharyngeal Cancer Patients, Front Oncol, 8 (2018) 589.

[49] T. Rieckmann, M. Kriegs, The failure of cetuximab-based de-intensified regimes for HPV-positive OPSCC: A radiobiologists perspective, Clinical and translational radiation oncology, 17 (2019) 47-50.

[50] S. Begum, D. Cao, M. Gillison, M. Zahurak, W.H. Westra, Tissue distribution of human papillomavirus 16 DNA integration in patients with tonsillar carcinoma, Clin Cancer Res, 11 (2005) 5694-5699.

[51] H. Husain, A. Psyrri, A. Markovic, T. Rampias, E. Pectasides, H. Wang, R. Slebos, W.G. Yarbrough, B. Burtness, C.H. Chung, Nuclear epidermal growth factor receptor and p16 expression in head and neck squamous cell carcinoma, The Laryngoscope, 122 (2012) 2762-2768.

[52] H.W. Lo, M.C. Hung, Nuclear EGFR signalling network in cancers: linking EGFR pathway to cell cycle progression, nitric oxide pathway and patient survival, British journal of cancer, 96 Suppl (2007) R16-20.

[53] K. Dittmann, C. Mayer, R. Kehlbach, H.P. Rodemann, Radiation-induced caveolin-1 associated EGFR internalization is linked with nuclear EGFR transport and activation of DNA-PK, Molecular cancer, 7 (2008) 69.

[54] K.B. Kang, C. Zhu, Y.L. Wong, Q. Gao, A. Ty, M.C. Wong, Gefitinib radiosensitizes stem-like glioma cells: inhibition of epidermal growth factor receptor-Akt-DNA-PK signaling, accompanied by inhibition of DNA double-strand break repair, Int J Radiat Oncol Biol Phys, 83 (2012) e43-52.

[55] M. Toulany, K.J. Lee, K.R. Fattah, Y.F. Lin, B. Fehrenbacher, M. Schaller, B.P. Chen, D.J. Chen, H.P. Rodemann, Akt promotes post-irradiation survival of human tumor cells through initiation, progression, and termination of DNA-PKcs-dependent DNA double-strand break repair, Mol Cancer Res, 10 (2012) 945-957.

[56] U. Raju, O. Riesterer, Z.Q. Wang, D.P. Molkentine, J.M. Molkentine, F.M. Johnson, B. Glisson, L. Milas, K.K. Ang, Dasatinib, a multi-kinase inhibitor increased radiation sensitivity by interfering with nuclear localization of epidermal growth factor receptor and by blocking DNA repair pathways, Radiotherapy and oncology : journal of the European Society for Therapeutic Radiology and Oncology, 105 (2012) 241-249.

[57] J. Liu, S.G. Kang, P. Wang, Y. Wang, X. Lv, Y. Liu, F. Wang, Z. Gu, Z. Yang, J.K. Weber, N. Tao, Z. Qin, Q. Miao, C. Chen, R. Zhou, Y. Zhao, Molecular mechanism of Gd@C(82)(OH)(22) increasing collagen expression: Implication for encaging tumor, Biomaterials, 152 (2018) 24-36.

[58] R. Weichselbaum, W. Dahlberg, J.B. Little, T.J. Ervin, D. Miller, S. Hellman, J.G. Rheinwald, Cellular X-ray repair parameters of early passage squamous cell carcinoma lines derived from patients with known responses to radiotherapy, British journal of cancer, 49 (1984) 595-601.

[59] B.J. Aubrey, G.L. Kelly, A. Janic, M.J. Herold, A. Strasser, How does p53 induce apoptosis and how does this relate to p53-mediated tumour suppression?, Cell Death Differ, 25 (2018) 104-113.

[60] T.C.G. Atlas, Comprehensive genomic characterization of head and neck squamous cell carcinomas, Nature, 517 (2015) 576-582.

884 [61] X. Xie, L. Piao, B.N. Bullock, A. Smith, T. Su, M. Zhang, T.N. Teknos, P.S. Arora, Q. Pan,
885 Targeting HPV16 E6-p300 interaction reactivates p53 and inhibits the tumorigenicity of
886 HPV-positive head and neck squamous cell carcinoma, Oncogene, 33 (2014) 1037-1046.

887 [62] G.S. Akerman, W.H. Tolleson, K.L. Brown, L.L. Zyzak, E. Mourateva, T.S. Engin, A.
888 Basaraba, A.L. Coker, K.E. Creek, L. Pirisi, Human papillomavirus type 16 E6 and E7
889 cooperate to increase epidermal growth factor receptor (EGFR) mRNA levels,
890 overcoming mechanisms by which excessive EGFR signaling shortens the life span of
891 normal human keratinocytes, Cancer Res, 61 (2001) 3837-3843.

892 [63] J. Shen, W. Xia, Y.B. Khotskaya, L. Huo, K. Nakanishi, S.O. Lim, Y. Du, Y. Wang, W.C.
893 Chang, C.H. Chen, J.L. Hsu, Y. Wu, Y.C. Lam, B.P. James, X. Liu, C.G. Liu, D.J. Patel, M.C. Hung,
894 EGFR modulates microRNA maturation in response to hypoxia through phosphorylation
895 of AGO2, Nature, 497 (2013) 383-387.

896 [64] A. Honegger, D. Schilling, H. Sultmann, K. Hoppe-Seyler, F. Hoppe-Seyler,
897 Identification of E6/E7-Dependent MicroRNAs in HPV-Positive Cancer Cells, Methods
898 Mol Biol, 1699 (2018) 119-134.

899 [65] J.A. McCaul, K.E. Gordon, F. Minty, J. Fleming, E.K. Parkinson, Telomere dysfunction
900 is related to the intrinsic radio-resistance of human oral cancer cells, Oral oncology, 44
901 (2008) 261-269.

902 [66] F.A. Gourronc, M.M. Robertson, A.K. Herrig, P.M. Lansdorp, F.D. Goldman, A.J.
903 Klingelhutz, Proliferative defects in dyskeratosis congenita skin keratinocytes are
904 corrected by expression of the telomerase reverse transcriptase, TERT, or by activation
905 of endogenous telomerase through expression of papillomavirus E6/E7 or the
906 telomerase RNA component, TERC, Experimental dermatology, 19 (2010) 279-288.

907 [67] A.J. Klingelhutz, S.A. Foster, J.K. McDougall, Telomerase activation by the E6 gene
908 product of human papillomavirus type 16, Nature, 380 (1996) 79-82.

909 [68] T. Kiyono, S.A. Foster, J.I. Koop, J.K. McDougall, D.A. Galloway, A.J. Klingelhutz, Both
910 Rb/p16INK4a inactivation and telomerase activity are required to immortalize human
911 epithelial cells, Nature, 396 (1998) 84-88.

912 [69] H. Mirghani, F. Amen, F. Moreau, J. Guigay, D.M. Hartl, J. Lacau St Guily, Oropharyngeal
913 cancers: relationship between epidermal growth factor receptor alterations and human
914 papillomavirus status, Eur J Cancer, 50 (2014) 1100-1111.

915 [70] A.N. Weaver, T.S. Cooper, M. Rodriguez, H.Q. Trummell, J.A. Bonner, E.L. Rosenthal,
916 E.S. Yang, DNA double strand break repair defect and sensitivity to poly ADP-ribose
917 polymerase (PARP) inhibition in human papillomavirus 16-positive head and neck
918 squamous cell carcinoma, Oncotarget, 6 (2015) 26995-27007.

919 [71] J.D. Guster, S.V. Weissleder, C.J. Busch, M. Kriegs, C. Petersen, R. Knecht, E. Dikomey,
920 T. Rieckmann, The inhibition of PARP but not EGFR results in the radiosensitization of
921 HPV/p16-positive HNSCC cell lines, Radiother Oncol, 113 (2014) 345-351.

Main Figures Legends

Fig. 1. EGFR expression in normal tonsillar epithelial tissues, OPSCC tissue samples. (A) Representative photomicrographs of EGFR immunohistochemistry in tonsillar tissues samples (a & c) surface epithelium, (b & d) crypt epithelium. The mean of EGFR H-score surface epithelium and crypt epithelium were 172 and 122.5, respectively. (B) Scattered dot plot of EGFR H scores obtained for EGFR immunohistochemical staining of normal tonsillar tissue samples. The median is indicated by a horizontal bar. (C) Representative photomicrographs of EGFR immunohistochemistry in four separate OPSCC tumour samples (a & b low power view, c & d high power view). The samples (a & c) were HPV-positive, and (b & d) were HPV-negative. The overall H-score for the tumour samples in a, b, c and d were 100, 300, 90 and 280, respectively. In all cases, the overlying nondysplastic epithelium served as intra-sectional referents. (D) Dot over box-and whisker plot of EGFR H-scores in OPSCC tumour samples. The median is indicated by a horizontal bar. (E) EGFR protein expression in a panel of HPV-negative and positive HNSCC cell lines. This figure is representative of 3 independent experiments. (F) Scattered dot plot of EGFR expression in HNSCC subtypes from TCGA dataset. EGFR expression in HPV-positive HNSCC tumours was significantly lower compared to HPV-negative HNSCC subset, analysed by unpaired t-test ($p<0.0452$). (G)Exogenous EGFR overexpression in HPV-negative SCC072 cell line was assessed by immunoblotting in pBabe-puro control (072 PBP) and overexpressing (072 EGFR) cells. Quantification of 3 independent experiments presented in bar-chart, un-paired t-test (**$p<0.003$). (H) Exogenous EGFR overexpression in HPV-positive SCC154 cell line was assessed by immunoblotting in pBabe-puro control (154 PBP) and overexpressing (154 EGFR) cells. Quantification of 3 independent experiments presented in bar-chart, un-paired t-test (***$p<0.002$). (I) EGFR subcellular localisation in HPV-negative 072 PBP and 072 EGFR was assessed by indirect immunofluorescence in the absence and presence of 100ng/ml of recombinant EGF for 10 min. (J) EGFR subcellular localisation in HPV-positive 154 PBP and 154 EGFR was assessed by indirect immunofluorescence in the absence and presence of 100ng/ml of recombinant EGF for 10 min. Representative images of 3 independent experiments were taken at 60x magnification. HN5 is HPV-negative HNSCC cell line; known for high endogenous EGFR expression was used as a positive control for all EGFR studies.

Fig. 2. EGFR overexpression regulates cellular proliferation, EGFR downstream activation and cell cycle differently in HPV-negative and positive HNSCC cell lines. (A) Cell proliferation was assessed daily by MTT assay over 5 days in HPV-negative 072 PBP and 072 EGFR. The data represent mean ± SEM of 3 independent experiments (***$p<0.0003$, **$p<0.001$ and ***$p<0.0007$ on day 3, 4 and 5, respectively) by two-way ANOVA. (B) Cell proliferation was assessed daily by MTT assay over 5 days in HPV-positive 154 PBP and 154 EGFR. The data represent mean ± SEM of 3 independent experiments (**$p<0.03$ and ***$p<0.001$on day 4 and 5, respectively) by two-way ANOVA. (C) A bar chart of cell cycle phases G0/G1, S and G2/M phase of HPV-negative 072 PBP and 072 EGFR cells stained with propidium iodide and analysed by FACS. A difference at G0/G1 determined by un-paired t-test, **$p<0.003$. (D) A bar chart of cell cycle phases G0/G1, S and G2/M phase of HPV-positive 154 PBP and 154 EGFR cells stained with propidium iodide and analysed by FACS. A difference at G0/G1 determined by un-paired t-test, ***$p<0.004$ and *$p<0.006$ at G2/M phase. (E) HPV-negative and positive PBP and EGFR cells were incubated in the presence of 100ng/ml of EGF for 30 min. Levels of phosphorylated EGFR at Tyr1068, phosphorylated STAT3 (Tyr705), phosphorylated AKT (Ser473) and phosphorylated ERK1/2 were determined by immunoblotting. Tubulin was served as a loading control. This immunoblot is representative of 3 independent experiments.

Fig. 3. EGFR overexpression in HPV-negative and positive HNSCC cells and response to radiation. (A) Clonogenic assay of HPV-negative 072 PBP and 072 EGFR cells. Cells were irradiated at 0,2,4 and 6Gy, fixed and stained after 7-10 days (B) Survival fraction of HPV-negative 072 PBP and 072 EGFR colonies after radiation (0,2,4 and 6Gy) normalised to the plating efficiency of non-irradiated control. Significant differences were analysed in 3 independent experiments by Two-way ANOVA ($p<0.0441$ at dose 4Gy). (C) Clonogenic assay of HPV-positive 154 PBP and 154 EGFR cells. Cells were irradiated at 0,2,4 and 6Gy, fixed and stained after 7-10 days (D) Survival fraction of HPV-positive 154 PBP and 154 EGFR colonies after radiation (0,2,4 and 6Gy) normalised to the plating efficiency of non-irradiated control. Significant differences were analysed in 3 independent experiments by Two-way ANOVA ($p<0.01$ at dose 4Gy and $p<0.02$ at dose 6Gy). (E) HPV-negative 072 PBP and 072 EGFR cells were irradiated at 4Gy and stained for gamma-H2AX foci at 30min and 24hrs post irradiation. (F) HPV-positive 154 PBP and 154 EGFR cells were irradiated at 4Gy and stained for gamma-H2AX foci at 30 min and 24 hrs post irradiation. ***$p<0.0005$ at 24 hrs (un-paired t-test). (G) Co-localisation of EGFR expression (red staining) and 53BP1 foci (green staining) was assessed by indirect immunofluorescence in HPV-negative 072 PBP and 072 EGFR in response to radiation dose 4Gy at 0hrs (Ctrl) at 1hr and 24hrs. Quantification of 3 independent experiments was analysed and presented by bar-chart *$p<0.01$ at 24 hrs (un-paired t-test). (H) Co-localisation of EGFR expression (red staining) and 53BP1 foci (green staining) was assessed by indirect immunofluorescence in HPV-positive 154 PBP and 154 EGFR in response to radiation dose 4Gy at 0hr (Ctrl), 1hr and 24hrs. Quantification of 3 independent experiments was analysed and presented by bar-chart ***$p<0.0005$ at 24 hrs (un-paired t-test). For E, F, G and H, A minimum of 100 foci at each time point was analysed and data is presented by bar chart. Error bars represent standard error of the mean (SEM) (n=3). Representative images of irradiated cells at 60X magnification. (I) HPV-negative 072 EGFR and 072 PBP cells were irradiated with 4Gy, collected and fixed at 30min,5 and 24hrs post-radiation. DNA was stained with EtBr for detecting comet tail. **$p<0.001$ at 24hrs (Two-way ANOVA). (J) HPV-positive 154 EGFR and 154 PBP cells were irradiated with 4Gy, collected and fixed at 30min, 5 and 24hrs post-radiation. DNA was stained with EtBr for detecting comet tail. *$p< 0.07$, ***$p<0.0001$ and ***$p<0.0001$ at 30 min, 5 and 24 hrs respectively (Two-way ANOVA).

Fig. 4. EGFR overexpression regulates cell cycle differently in HPV-negative and positive HNSCC cell lines. (A) HPV-negative 072 PBP and 072 EGFR cells were treated with 2μM Gefitinib or 4Gy radiation and in combination for 24hrs, cell cycle was analysed by PI staining followed by FACS. Representative PI histograms showing number of cells in G1 phase (left peak), G2 phase (right peak) as well as S phase and sub-G1 phase. Bar charts represent ratio of cell cycle phases (n=3). (B) Quantification of cells in G2 cell cycle phase after treatment, error bars indicate standard error of the mean (SEM) (n = 3). (C) Quantification of cells in Sub G1 cell cycle phase after treatment, error bars indicate SEM (n = 3). (D) HPV-positive 154 PBP and 154 EGFR cells were treated with 2μM Gefitinib or 4Gy radiation and in combination for 24hrs, cell cycle was analysed by PI staining followed by FACS. Representative PI histograms showing number of cells in G1 phase (left peak), G2 phase (right peak) as well as S phase and sub-G1 phase. Bar charts represent ratio of cell cycle phases (n=3). (E) Quantification of cells in G2 cell cycle phase after treatment, error bars indicate standard error of the mean (SEM) (n = 3). (F) Quantification of cells in Sub G1 cell cycle phase after treatment, error bars indicate SEM (n = 3).

Fig. 5. EGFR overexpression affects DNA damage repair proteins in HPV-negative and positive HNSCC cell lines. (A) HPV-negative 072 PBP {C} and 072 EGFR {E} cells were irradiated with 4Gy and lysates collected at 30min, 2 and 5hrs. Levels of phosphorylated EGFR, Ku80 and Rad51 were determined by immunoblotting (B) Quantifications of 3 independent experiments for protein levels of RAD51 and Ku80 in both HPV-negative 072 PBP and 072 EGFR. Significant differences in RAD51 and Ku80 protein levels were determined by two-way ANOVA. (C) HPV-positive 154 PBP {C} and 154 EGFR {E} cells were irradiated with 4Gy and lysates collected at 30min, 2 and 5hrs. Levels of phosphorylated EGFR, Ku80 and Rad51 were determined by immunoblotting. (D) Quantifications of 3 independent experiments for protein levels of RAD51 and Ku80 in HPV-positive 154 PBP and 154 EGFR. Significant differences in RAD51 and Ku80 protein levels were determined by two-way ANOVA. (E) HPV-negative 072 PBP {C} and 072 EGFR {E} cells were irradiated with 4Gy and lysates collected at 30min, 2 and 5hrs. Levels of EGFR, DNA-PKcs and phosphorylated Akt Ser437 were determined by immunoblotting. (F) Quantifications of 3 independent experiments for protein levels of DNA-PKcs and phosphorylated Akt Ser437 HPV-negative 072 PBP and 072 EGFR. Significant differences in DNA-PKcs and phosphorylated Akt Ser437 protein levels were determined by two-way ANOVA. (G) HPV-positive 154 PBP {C} and 154 EGFR {E} cells were irradiated with 4Gy and lysates collected at 30min, 2 and 5hrs. Levels of EGFR, DNA-PKcs and phosphorylated Akt Ser437 were determined by immunoblotting. (H) Quantifications of 3 independent experiments for protein levels of DNA-PKcs and phosphorylated Akt Ser437 HPV-positive 154 PBP and 154 EGFR. Significant differences in DNA-PKcs and phosphorylated Akt Ser437 protein levels were determined by two-way ANOVA. (I) HPV-positive 154 PBP {C} and 154 EGFR {E} cells were irradiated with 4Gy, lysates were collected at 30min, 2, 5 and 24hrs post-radiation and analysed by immunoblotting. Quantification of $p21^{waf1/cip1}$ from 3 independent experiments represented by bar-chart. Significant differences were determined by Two-way ANOVA, $p<0.05$, $p<0.003$ and $p<0.005$ at 30 min, 2 and 5 hrs respectively. (J) HPV-E6 expression in 154 PBP and 154 EGFR was measured by qRT-PCR in 3 independent RNA extractions. Statistical analysis was performed by un-paired t-test ($p<0.001$).

Fig. 6. EGFR overexpression in HPV-positive SCC154 xenograft model affects tumour volume in response to radiation. (A) The tumour volume of HPV-positive 154 PBP xenograft model (control) and radiated with 18Gy (Rad) n=11-12. The average tumour volumes ± SEM are presented by line graph. (B) The tumour volume of HPV-positive 154 EGFR overexpressing xenograft model (control) and radiated with 18Gy (Rad) n=11-12. The average tumour volumes ± SEM are presented by line graph. Statistical significance was determined by un-paired t-test ($p<0.03$ and $p<0.001$ at day 6 and day 8 treatment. (C) Scattered dot blot of proliferation marker (Ki67) in HPV-positive 154 EGFR overexpressing cells. The expression levels were analysed in 18-25 different tumour regions in the (control) versus (radiated) groups. Statistical significance was determined by unpaired *t*-test ($p<0.0001$). Representative immunohistochemistry (IHC) images of 154 EGFR xenograft tumour tissues of both (control) and (radiated) groups for Ki67 staining. (D) Scattered dot blot of Collagen-trichome staining of fibrotic tissues in HPV-positive 154 EGFR overexpressing cells. The expression levels were analysed in 15-20 different tumour regions in the (control) versus (radiated) groups. Statistical significance was determined by unpaired *t*-test ($p<0.0001$). Representative immunohistochemistry (IHC) images of 154 EGFR xenograft tumour tissues of both (control) and (radiated) groups for trichrome staining.

Fig. 7. Proposed model for the role of EGFR overexpression in HPV-positive HNSCC cells. A schematic presentation of potential mechanisms by which EGFR overexpression could regulate HPV-positive response to radiation-induced DNA damage, where reduced AKT signalling results in impaired recruitment of DNA-PKcs leading to impairment of NHEJ repair pathway, reduced DSB repair and increased radiosensitivity. A novel role of EGFR overexpression in reducing HPV E6 expression, suggests a possible mechanism in restoration of p53 and induction of cell death.

Figure 1

A

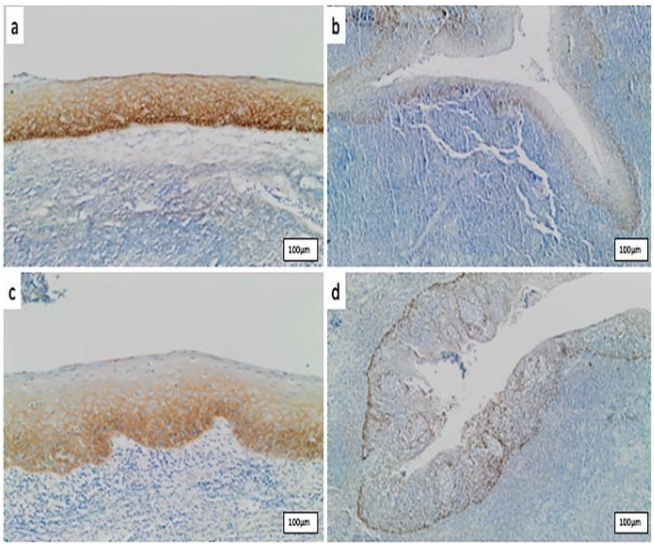

B

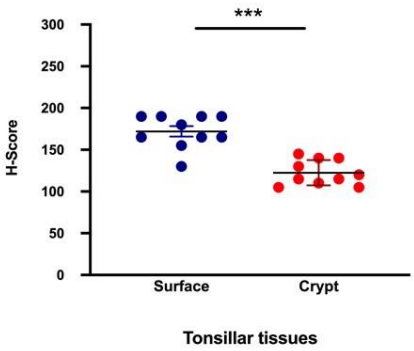

1075

Figure 1 continued I

C

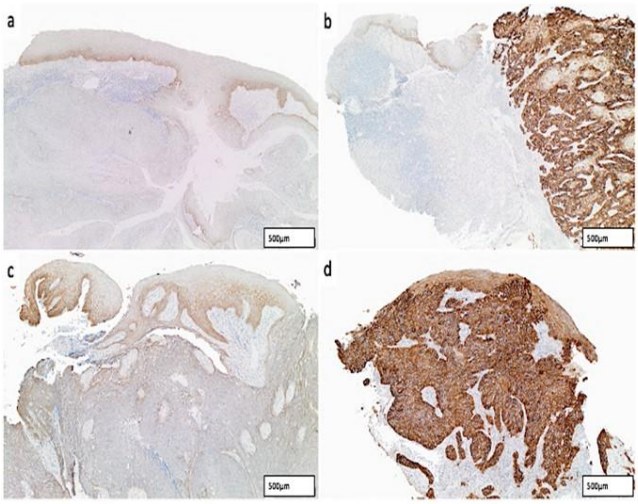

D

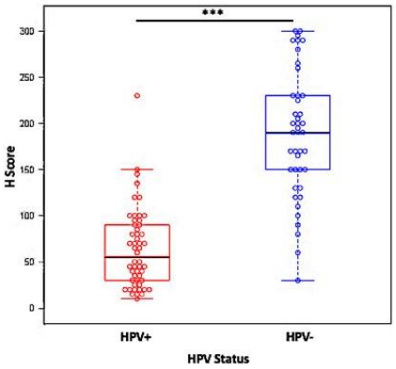

1076

Figure 1 continued II

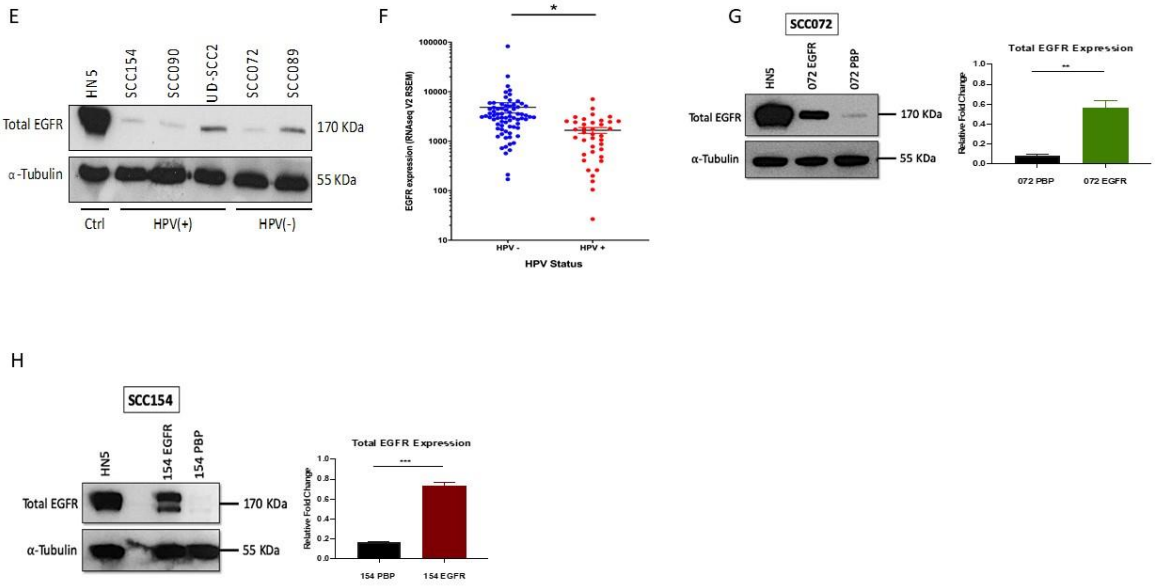

1077

Figure 1 continued II

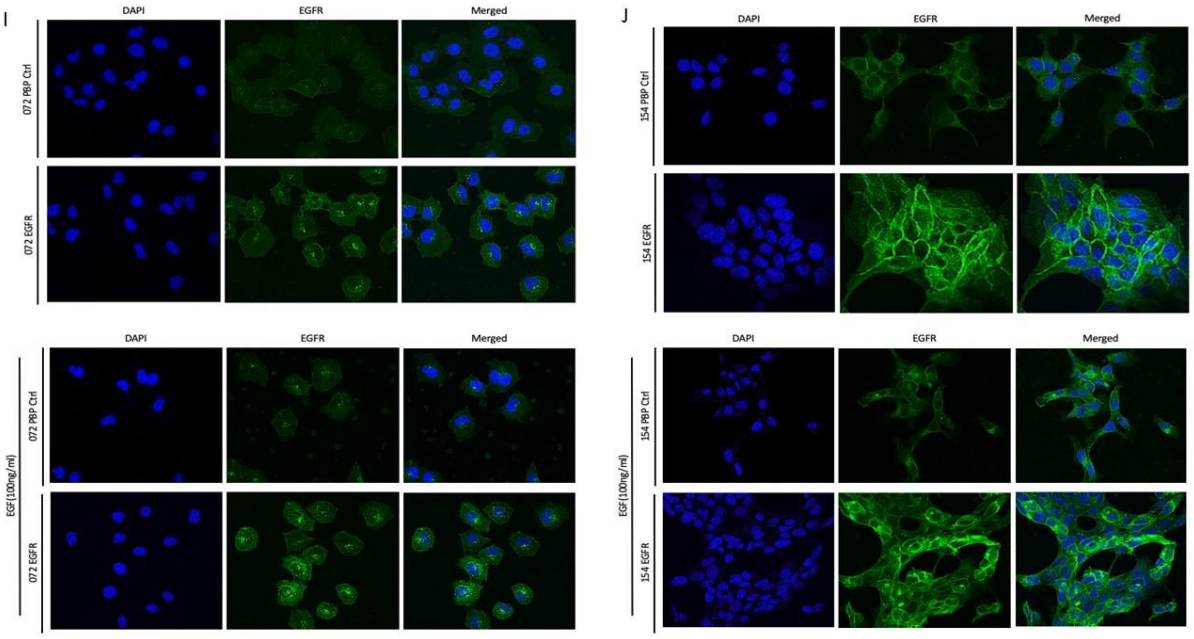

1078

Figure 2

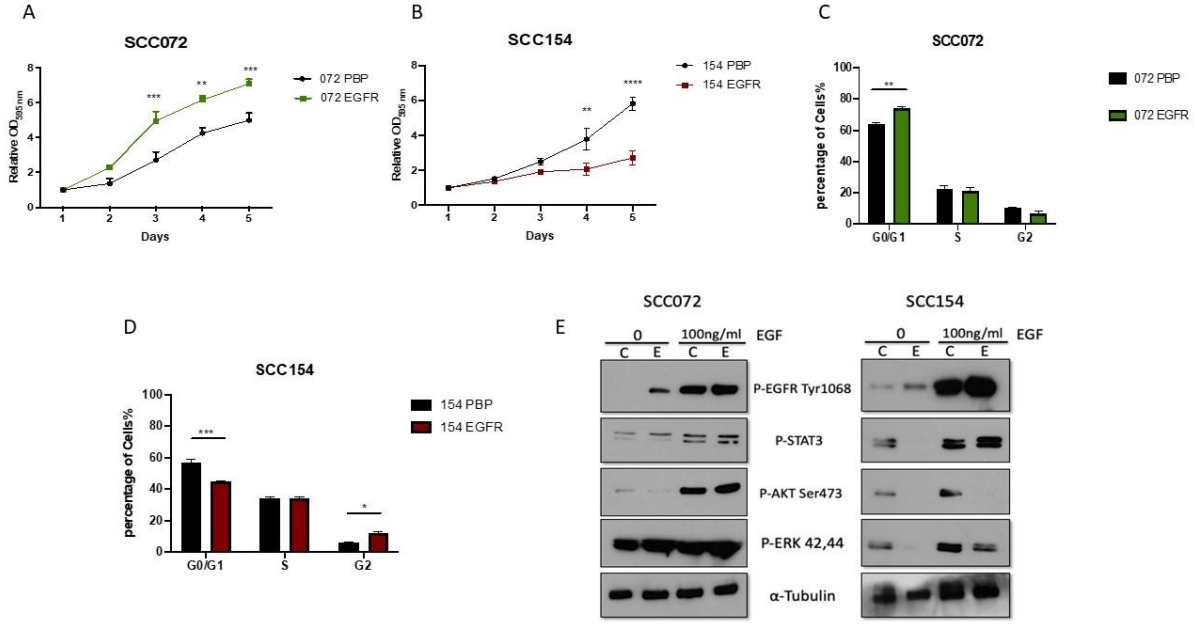

1079

Figure 3

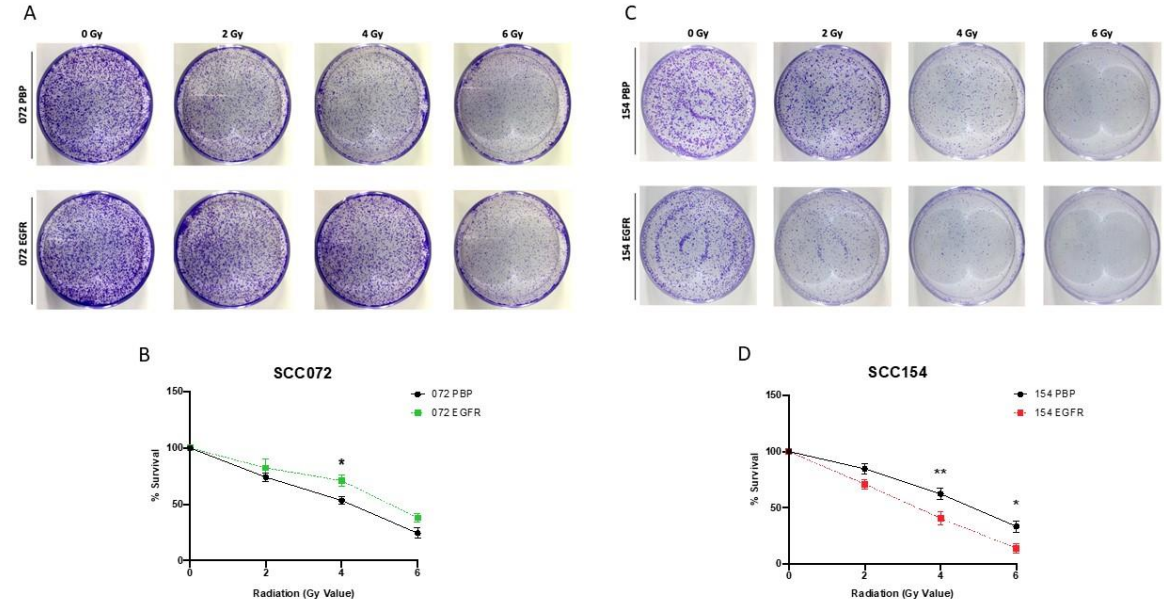

1080

Figure 3 continued I

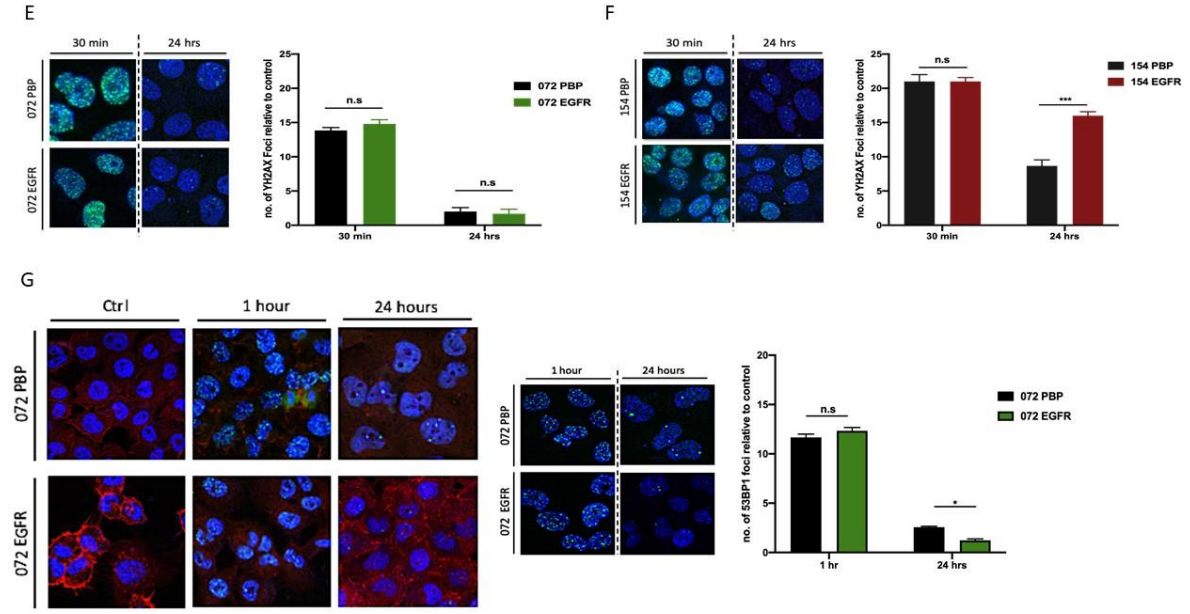

1081

Figure 3 continued II

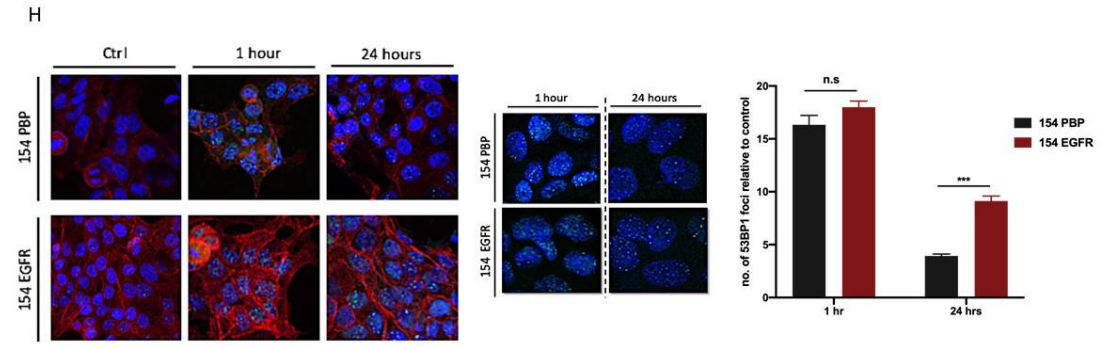

1082

Figure 3 continued III

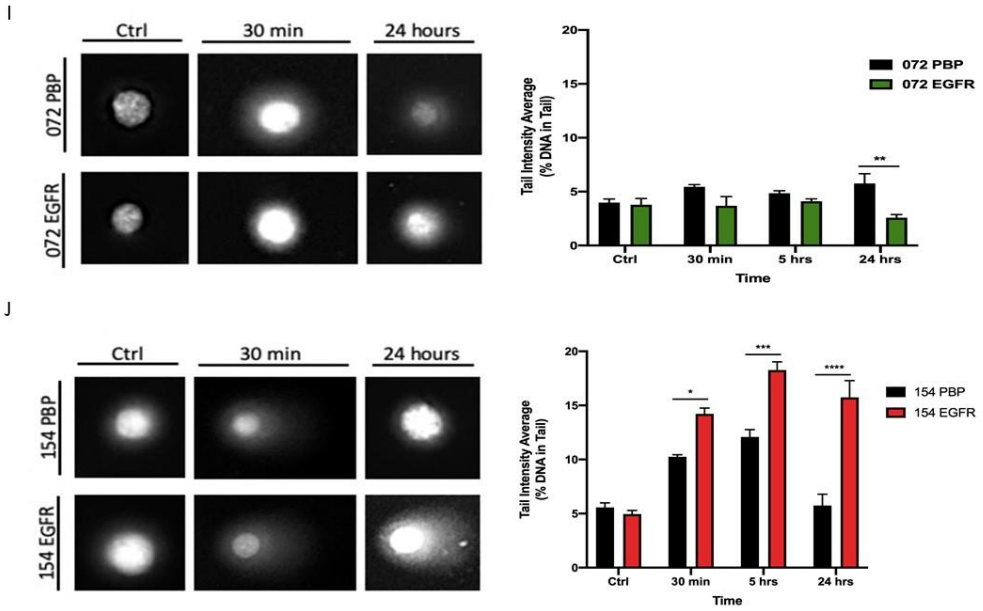

1083

Figure 4

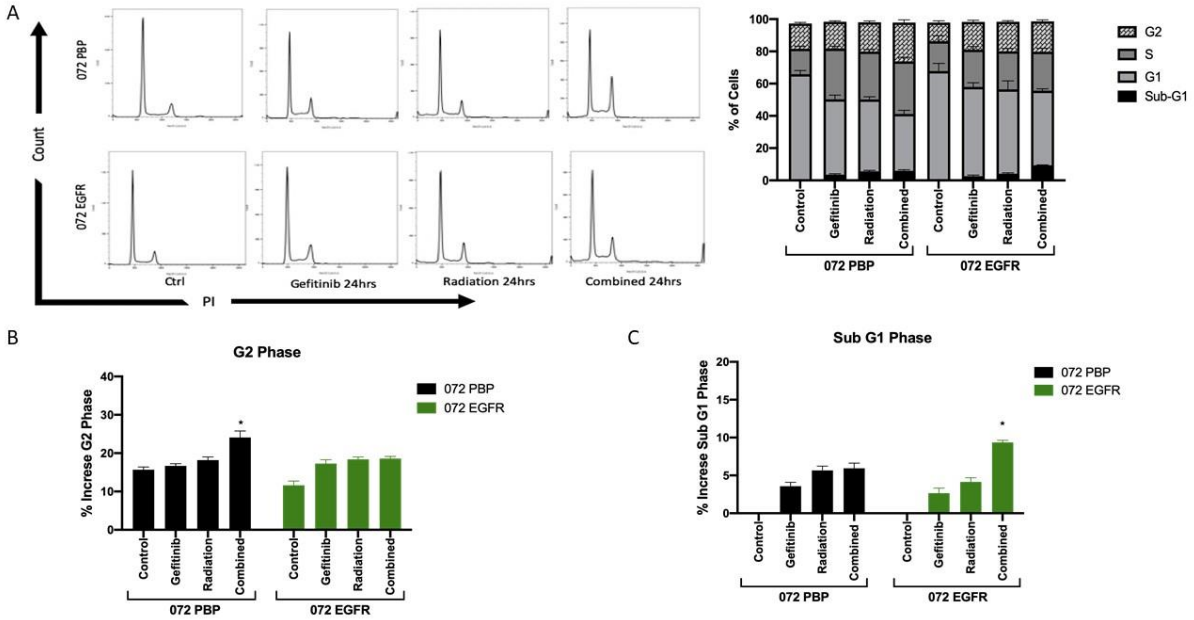

1084

Figure 4 continued

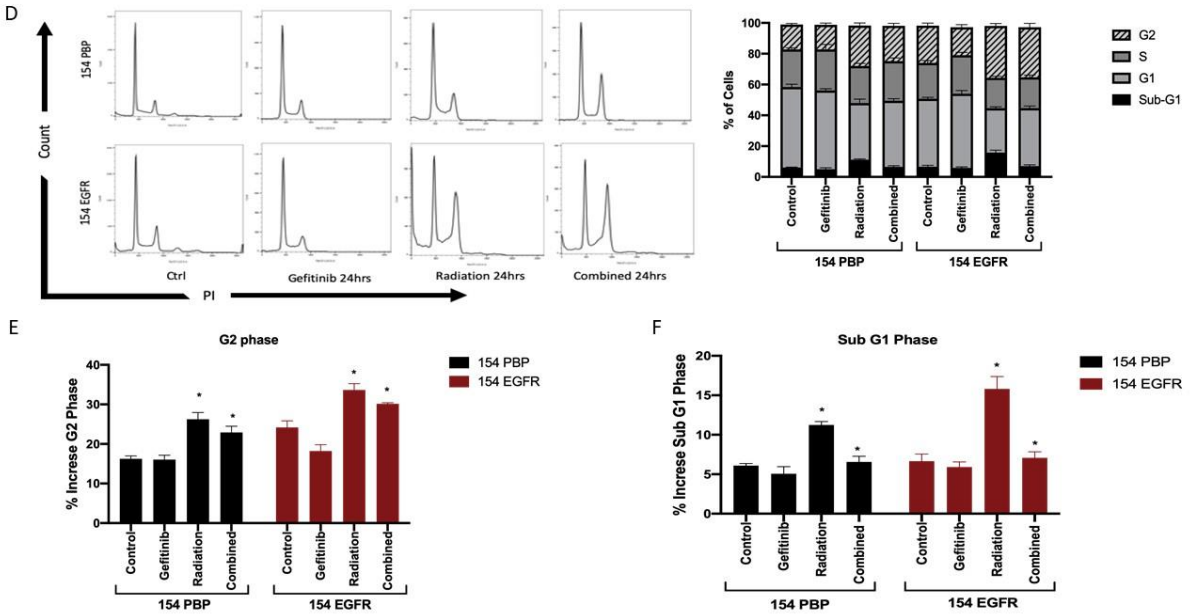

1085

Figure 5

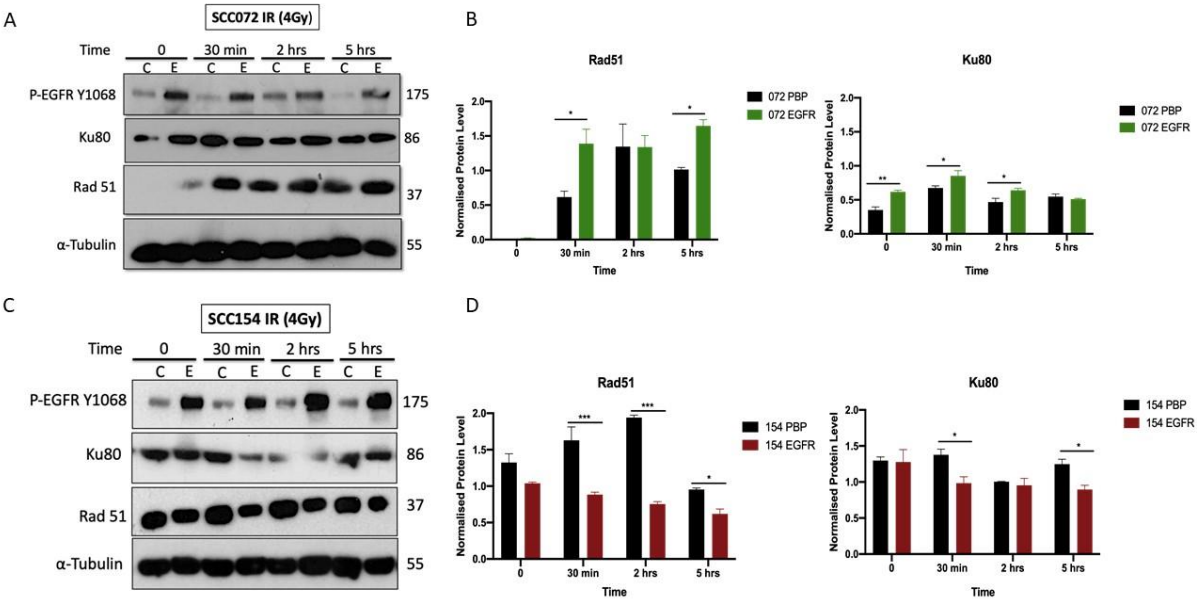

1086

Figure 5 continued I

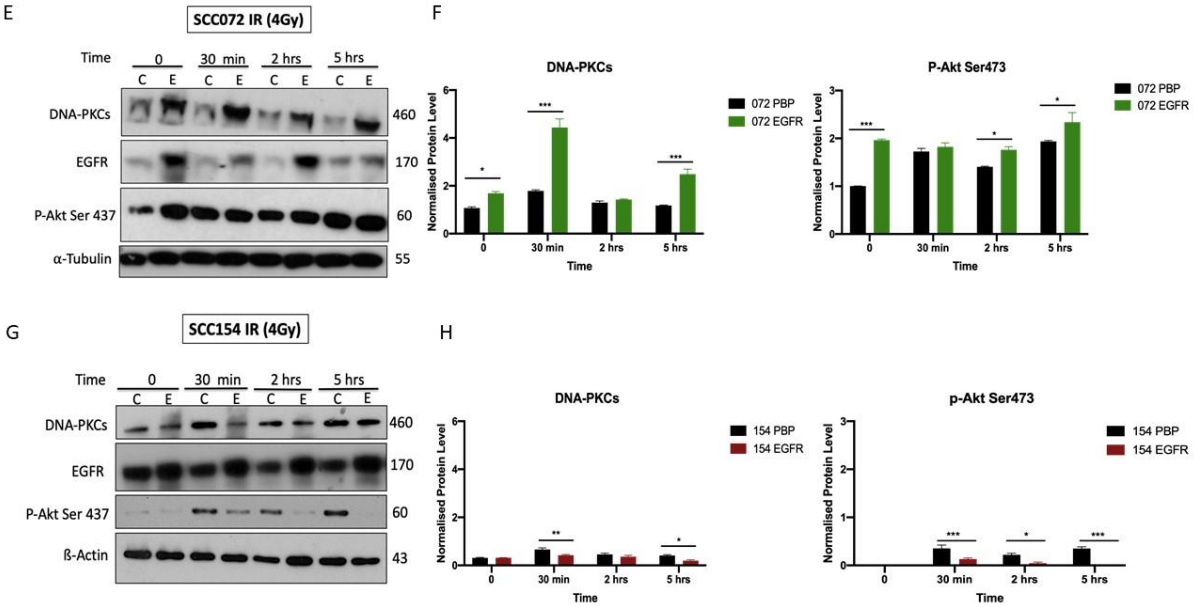

1087

Figure 5 continued II

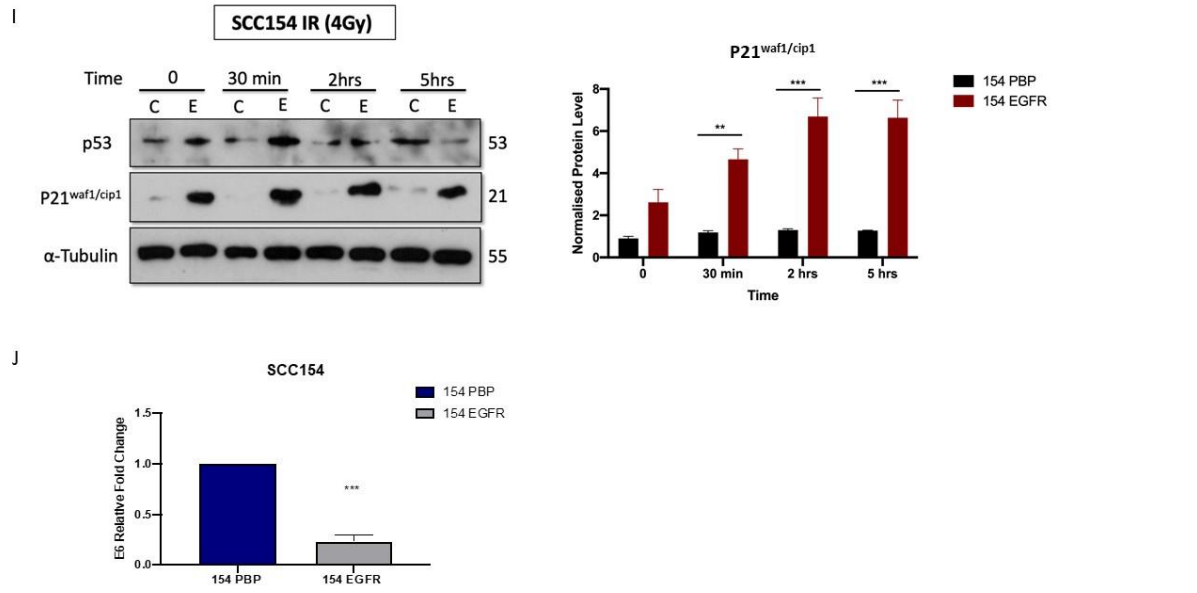

1088

Figure 6

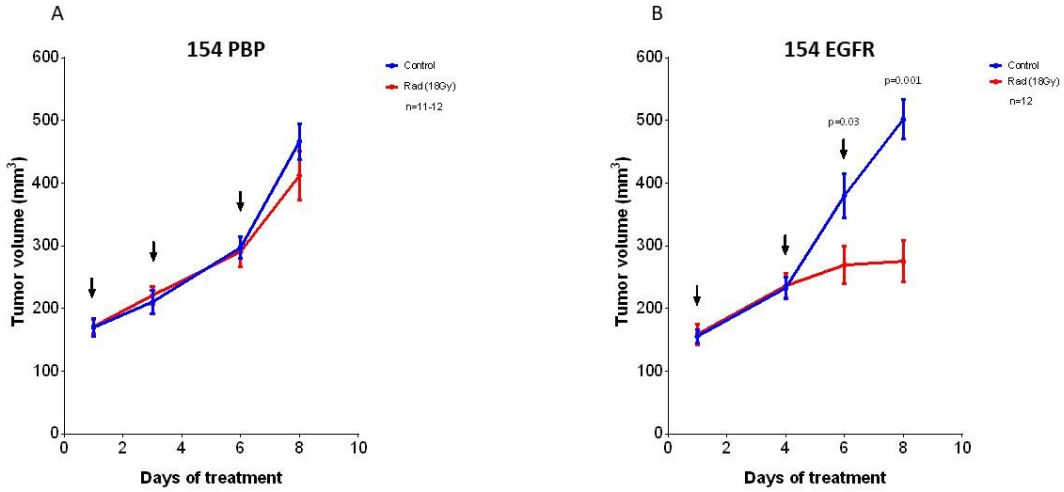

1089

Figure 6 C

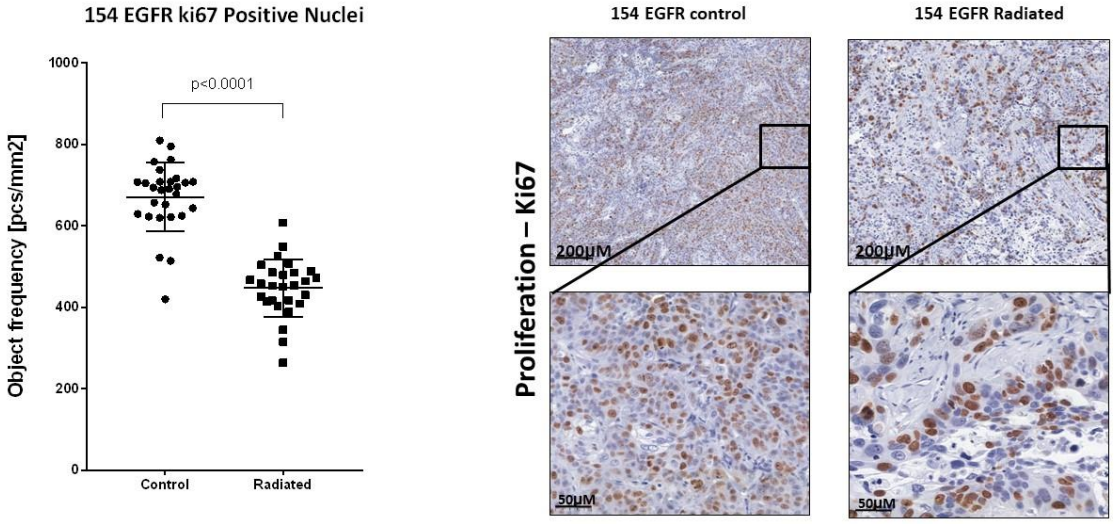

1090

Figure 6 D

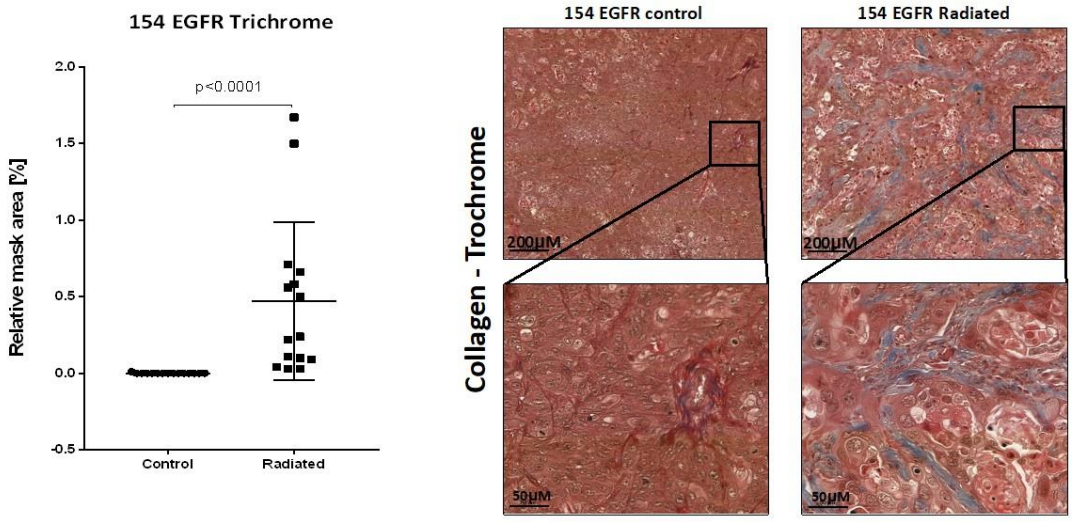

1091

Figure 7

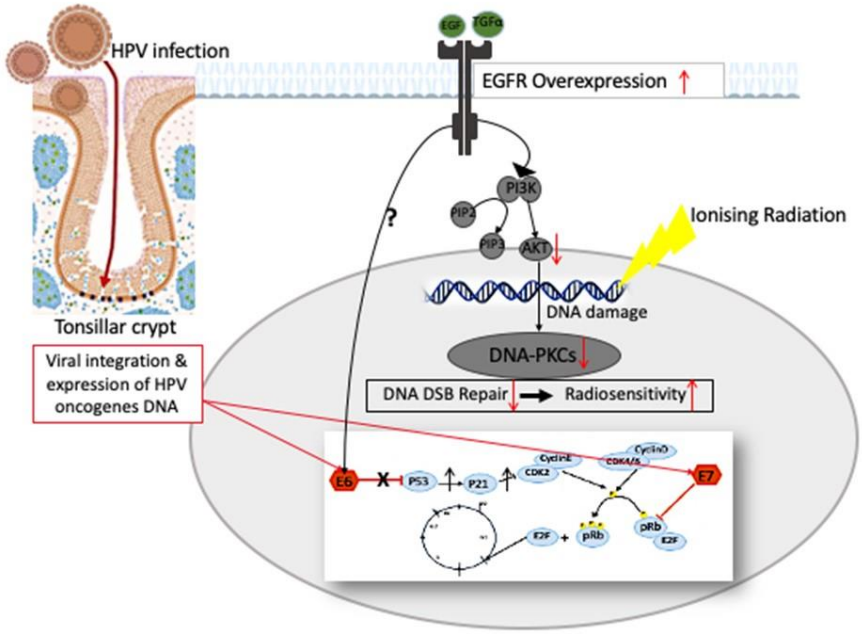

1092